Quark models of the nucleon *

Roelof Bijker †
Instituto de Ciencias Nucleares,
Universidad Nacional Autónoma de México,
A.P. 70-543, 04510 México, Distrito Federal, México

Abstract

In these lecture notes I discuss some general aspects of quark models of baryons. In spite of the successes of the quark model in describing masses, magnetic moments, electromagnetic and strong couplings, there are some systematic discrepancies with the experimental data that cannot be explained in any quark model based on valence quarks only.

In the first part I review some general features of quark models based on three valence quarks, and in the second part I present an unquenched quark model for baryons in which the effects of sea quarks are taken into account in an explicit form via a microscopic, QCD-inspired, creation mechanism of the quark-antiquark pairs. In this approach, the contribution of the quark-antiquark pairs can be studied for any inital baryon and for any flavor of the $q\bar{q}$ pairs ($u\bar{u}$, $d\bar{d}$ and $s\bar{s}$). It is shown that, whereas the inclusion of the $q\bar{q}$ pairs (or hadron loops) does not affect the baryon magnetic moments, it automatically leads to an excess of $\bar{d}$ over $\bar{u}$ in the proton and introduces a sizeable contribution of orbital angular momentum to the spin of the proton.

*Lectures notes, 'VII Escuela Mexicana de Física Nuclear', México, Distrito Federal, June 20 - 28, 2011

†E-mail: bijker@nucleares.unam.mx

Contents

1 Introduction

The structure of the nucleon is of fundamental importance in nuclear and particle physics. The first indication that the nucleon is not a point particle but has an internal structure came from the measurement of the anomalous magnetic moment of the proton in the 1930's [1], which was determined to be about 2.5 times as large as one would expect for a spin 1/2 Dirac particle (the actual value is 2.793 [2]). The finite size of the proton was measured in the 1950's in electron scattering experiments at SLAC to be ~ 0.8 fm [3] (compared to the current value of 0.877 ± 0.007 fm [2]). The first evidence for point-like constituents (quarks) inside the proton was found in deep-inelastic-scattering experiments in the late 1960's by the MIT-SLAC collaboration [4] which eventually, together with many other developments, would lead to the formulation of QCD in the 1970's as the theory of strongly interacting particles. The complex structure of the proton manifested itself once again in recent polarization transfer experiments [5] which showed that the ratio of electric and magnetic form factors of the proton exhibits a dramatically different behavior as a function of the momentum transfer as compared to the phenomenon of form factor scaling obtained from the Rosenbluth separation method [6].

The building blocks of atomic nuclei, the nucleons, are composite extended objects. High precision data on the properties of the nucleon and its excited states, collectively known as baryons, have been accumulated over the past years at Jefferson Laboratory, MIT-Bates, LEGS at BNL, MAMI in Mainz, ELSA in Bonn and GRAAL in Grenoble [7]. To first approximation, the internal structure of the nucleon at low energy can be ascribed to three bound constituent quarks qqq. The baryons are accommodated into flavor singlets, octets and decuplets [8]. Each flavor multiplet consists of families of baryons characterized by their isospin and strangeness.

In these lecture notes, I discuss some general features of quark models based on three valence quarks. As a specific example, I review some properties of a stringlike collective model in which the baryons (three-quark configurations) are interpreted as rotations and vibrations of the strings. In spite of the successes of quark models in general in describing masses, magnetic moments, electromagnetic and strong couplings, there are some systematic discrepancies with the experimental data on electromagnetic and strong couplings that cannot be explained in any quark model based on valence quarks only. Additional evidence for higher Fock components in the baryon wave function (such as $qqq-q\bar{q}$ configurations) comes from measurements of the $\bar{d}/\bar{u}$ asymmetry in the nucleon sea [9, 10] and parity-violating electron scattering experiments which report a nonvanishing strange quark contribution, albeit small, to the charge and magnetization distributions [11, 12]. In the second part, I present an unquenched quark model for baryons in which the effects of sea quarks are taken into account in an explicit form via a microscopic, QCD-inspired, creation mechanism of the quark-antiquark pairs ($u\bar{u}$, $d\bar{d}$ and $s\bar{s}$). It is shown that, while the inclusion of the $q\bar{q}$ pairs (or hadron loops) does not affect the baryon magnetic moments, it automatically leads to an excess of $\bar{d}$ over $\bar{u}$ in the proton and introduces a sizeable contribution of orbital angular momentum to the spin of the proton.

The outline of these lecture notes is as follows. In Section 2 some general aspects of

multiquark states are discussed. In Section 3 I disscuss some general features of quark models and, in particular, review some properties of a stringlike collective model and its application to baryon resonances (the nucleon and its excited states). In Section 4 I introduce the unquenched quark model with application to magnetic moments, and the flavor and spin content of the nucleon. The summary and conclusions are presented in Section 5. Some technical details concerning the spin and flavor wave functions are discussed in the appendices.

2 Multiquark states

Multiquark states depend both on the internal degrees of freedom of color, flavor and spin and the spatial degrees of freedom. The classification of the states will be studied from symmetry principles without introducing an explicit dynamical model. The construction of the classification scheme is guided by two conditions: the total multiquark wave function should be a color singlet and should be antisymmetric under any permutation of the quarks.

The internal degrees of freedom are taken to be the three light flavors u, d, s with spin $S = 1/2$ and three possible colors r, g, b. The internal algebraic structure of the constituent parts consists of the usual spin-flavor (sf) and color (c) algebras

$$\mathcal{G}_{\rm sfc} = SU_{\rm sf}(6) \otimes SU_{\rm c}(3) \ , \tag{2.1}$$

where the $SU_{\rm c}(3)$ algebra decribes the (unitary) transformations among the three different colors. The spin-flavor algebra can be decomposed into

$$SU_{\rm sf}(6) \supset SU_{\rm f}(3) \otimes SU_{\rm s}(2) \ , \tag{2.2}$$

where the $SU_{\rm f}(3)$ algebra decribes the transformations among the three different flavors and $SU_{\rm s}(2)$ among the two spin states of the quarks. The flavor algebra in turn can be decomposed into

$$SU_{\rm f}(3) \supset SU_{\rm I}(2) \otimes U_{\rm Y}(1) \ , \tag{2.3}$$

where I denotes the isospin and Y the hypercharge of the quarks. The states of a given flavor multiplet can be labeled by isospin I, I_3 and hypercharge Y. The electric charge is given by the Gell-Mann-Nishijima relation

$$Q \ = \ I_3 + \frac{Y}{2} \ = \ I_3 + \frac{B+\mathcal{S}}{2} \ , \tag{2.4}$$

where B denotes the baryon number and $\mathcal{S}$ the strangeness. The quantum numbers of the three light quarks and antiquarks are given in Table 1. The quarks have baryon number $B = \frac{1}{3}$ and spin and parity $S^P = \frac{1}{2}^+$ whereas the antiquarks have $B = -\frac{1}{3}$ and $S^P = \frac{1}{2}^-$.

I shall make use of the Young tableau technique [13] to construct the allowed representations of $SU(n)$ for the multiquark system with $n = 2$, 3 and 6 for the spin, flavor (or

Table 1: Quantum number of the quarks and antiquarks

	B	S^P	I	I_3	$\mathcal{S}$	Y	Q
u	$\frac{1}{3}$	$\frac{1}{2}^+$	$\frac{1}{2}$	$\frac{1}{2}$	0	$\frac{1}{3}$	$\frac{2}{3}$
d	$\frac{1}{3}$	$\frac{1}{2}^+$	$\frac{1}{2}$	$-\frac{1}{2}$	0	$\frac{1}{3}$	$-\frac{1}{3}$
s	$\frac{1}{3}$	$\frac{1}{2}^+$	0	0	-1	$-\frac{2}{3}$	$-\frac{1}{3}$
$\bar{u}$	$-\frac{1}{3}$	$\frac{1}{2}^-$	$\frac{1}{2}$	$-\frac{1}{2}$	0	$-\frac{1}{3}$	$-\frac{2}{3}$
$\bar{d}$	$-\frac{1}{3}$	$\frac{1}{2}^-$	$\frac{1}{2}$	$\frac{1}{2}$	0	$-\frac{1}{3}$	$\frac{1}{3}$
$\bar{s}$	$-\frac{1}{3}$	$\frac{1}{2}^-$	0	0	1	$\frac{2}{3}$	$\frac{1}{3}$

color) and spin-flavor degrees of freedom, respectively. The fundamental representation of $SU(n)$ is denoted by a box. The Young tableaux of $SU(n)$ are labeled by a string of n numbers $[f_1, f_2, \ldots, f_n]$ with $f_1 \geq f_2 \geq \ldots \geq f_n$ where f_i denotes the number of boxes in the i-th row. The labels which are zero are usually not written explicitly. The quarks transform as the fundamental representation [1] under $SU(n)$, whereas the antiquarks transform as the conjugate representation $[1^{n-1}]$ under $SU(n)$ [14, 15]. As a consequence, the three quarks belong to the flavor triplet [1] of $SU_{\rm f}(3)$ and the three antiquarks to the anti-triplet [11]. Instead of classifying the $SU(3)$ flavor multiplets by their Young tableau $[f_1, f_2, f_3]$ one also uses the labels $(p, q) = (f_1 - f_2, f_2 - f_3)$ or the dimension of the representation $\dim_{(p,q)} = (p+1)(q+1)(p+q+2)/2$. A standard representation of $SU(3)$ multiplets is that of a socalled weight diagram in the I_3-Y plane (see Table 1 and Figure 1).

The spin of the quarks and the antiquarks is determined by the representation $[f_1, f_2]$ of $SU_{\rm s}(2)$ as $S = \frac{f_1 - f_2}{2}$. The spin-flavor classification of a single quark and antiquark is given by

$$
\begin{array}{lccccc}
 & SU_{\rm sf}(6) & \supset & SU_{\rm f}(3) & \otimes & SU_{\rm s}(2) \\
\text{quark} & [1] & \supset & [1] & \otimes & [1] \\
 & \square & \supset & \square & \otimes & \square \\
\text{antiquark} & [11111] & \supset & [11] & \otimes & [1] \\
 & \begin{array}{c}\square\\\square\\\square\\\square\\\square\end{array} & \supset & \begin{array}{c}\square\\\square\end{array} & \otimes & \square
\end{array}
\tag{2.5}
$$

The spin-flavor states of multiquark systems can be obtained by taking the outer product of the representations of the quarks and/or antiquarks.

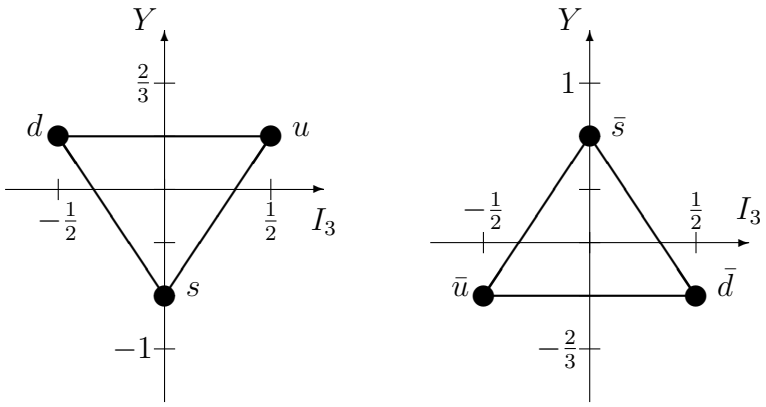

Figure 1: Quark triplet with $(p,q) = (1,0)$ (left) and antiquark anti-triplet with $(p,q) = (0,1)$ (right)

The requirement that physical states be color singlets, makes the quarks (or antiquarks) cluster into three-quark triplets (qqq baryons), quark-antiquark pairs ($q\bar{q}$ mesons) or products thereof. In general, the multiquark configurations can be expressed as

$$q^{3m+n}\bar{q}^{3k+n} \ , \tag{2.6}$$

which reduces to qqq baryons for $m = 1$ and $k = n = 0$, to $\bar{q}\bar{q}\bar{q}$ antibaryons for $m = n = 0$ and $k = 1$, and to $q\bar{q}$ mesons for $m = k = 0$ and $n = 1$.

2.1 qqq Baryons

The nucleon is not an elementary particle, but it is generally viewed as a confined system of three constituent quarks interacting via gluon exchange. Effective models of the nucleon and its excited states (or baryon resonances) are based on three constituent parts that carry the internal degrees of freedom of spin, flavor and color, but differ in their treatment of radial (or orbital) excitations. Here I discuss the internal degrees of freedom of qqq baryons.

The allowed spin, flavor and spin-flavor states are obtained by standard group theoretic techniques [13, 14, 15]. For example, the total spin of the three-quark system is obtained by coupling the three $\frac{1}{2}$ spins to give $S = \frac{3}{2}$ and $S = \frac{1}{2}$ (twice). In general, the spin, flavor and spin-flavor states of the three-quark system are obtained by taking the product

$$\begin{aligned} &[1] \otimes [1] \otimes [1] = [3] \oplus 2\,[21] \oplus [111] \\ &\square \otimes \square \otimes \square = \square\!\square\!\square \oplus 2 \begin{array}{|c|c|}\hline \ \ & \\ \hline \end{array} \oplus \begin{array}{|c|}\hline \ \ \\ \hline \ \ \\ \hline \end{array} \end{aligned} \tag{2.7}$$

where each of the boxes on the left-hand side denotes a quark.

An important ingredient in the construction of baryon wave function is the permutation symmetry between the quarks. If some of the constituent parts are identical one

must construct states and operators that transform according to the representations of the permutation group (either S_3 for three identical parts or S_2 for two identical parts). Here I discuss states that have good permutation symmetry among the three quarks S_3. These states form a complete basis which can be used for any calculation of baryon properties. The permutation symmetry of the three-quark system is characterized by the S_3 Young tableaux [3] (symmetric), [21] (mixed symmetric) and [111] (antisymmetric) or, equivalently, by the irreducible representations of the point group D_3 (which is isomorphic to S_3) as A_1, E and A_2, respectively. For notational purposes the latter is used to label the discrete symmetry of the baryon wave functions. The corresponding dimensions are 1, 2 and 1.

For the coupling of the spins, the antisymmetric representation [111] in Eq. (2.7) does not occur, since the representations of $SU_{\rm s}(2)$ can have at most two rows. This means that the spin of the three-quark system can be either $S = \frac{f_1 - f_2}{2} = \frac{3}{2}$ (Young tableau [3]) or $S = \frac{1}{2}$ (Young tableau [21]) with permutation symmetry A_1 and E, respectively. The dimension of the spin S is given by the number of spin projections $2S + 1$. The allowed spin, flavor and spin-flavor states are summarized in Table 2. The allowed flavor states are [3], [21] and [111] which are usually denoted by their dimensions as 10 (decuplet), 8 (octet) and 1 (singlet), respectively. The corresponding point group symmetries are A_1, E and A_2. Finally, the spin-flavor states are denoted by their dimensions as [56], [70] and [20] with symmetries A_1, E and A_2, respectively.

The spin and flavor content of each spin-flavor multiplet is given by the decomposition of the representations of $SU_{\rm sf}(6)$ into those of $SU_{\rm f}(3) \otimes SU_{\rm s}(2)$

$$\begin{aligned} [56] &\supset {}^2 8 \oplus {}^4 10 \,, \\ [70] &\supset {}^2 8 \oplus {}^4 8 \oplus {}^2 10 \oplus {}^2 1 \,, \\ [20] &\supset {}^2 8 \oplus {}^4 1 \,, \end{aligned} \tag{2.8}$$

where the superscript denotes $2S + 1$. For example, the symmetric representation [56]

Table 2: Allowed color, spin, flavor and spin-flavor baryon states

	q^3	Dimension	$S_3 \sim D_3$
color	[111]	singlet	A_2
spin	[3]	4	A_1
	[21]	2	E
flavor	[3]	decuplet	A_1
	[21]	octet	E
	[111]	singlet	A_2
spin-flavor	[3]	56	A_1
	[21]	70	E
	[111]	20	A_2

Table 3: Classification of ground state baryons according to $SU_{\rm f}(3) \supset SU_{\rm I}(2) \otimes U_{\rm Y}(1)$

			I	Y	Q
$J^P = \frac{1}{2}^+$ octet	Nucleon	N	$\frac{1}{2}$	1	0,1
	Sigma	Σ	1	0	–1,0,1
	Lambda	Λ	0	0	0
	Xi	Ξ	$\frac{1}{2}$	–1	–1,0
$J^P = \frac{3}{2}^+$ decuplet	Delta	Δ	$\frac{3}{2}$	1	–1,0,1,2
	Sigma	Σ^*	1	0	–1,0,1
	Xi	Ξ^*	$\frac{1}{2}$	–1	–1,0
	Omega	Ω	0	–2	–1

contains an octet with $S = \frac{1}{2}$ characterized by $(p, q) = (1, 1)$, and a decuplet with $S = \frac{3}{2}$ labeled by $(p, q) = (3, 0)$. In the absence of orbital excitations the parity of the qqq baryons is positive $P = +$.

In Table 3 I present the classification of the baryon flavor octet and decuplet in terms of the isospin I and the hypercharge Y according to the decomposition of the flavor symmetry $SU_{\rm f}(3)$ into $SU_{\rm I}(2) \otimes U_{\rm Y}(1)$. The nucleon and Δ are nonstrange baryons with $\mathcal{S} = 0$, whereas the Σ, Λ, Ξ and Ω hyperons carry strangeness $\mathcal{S} = -1$, -1, -2 and -3, respectively. The flavor singlet [111] with A_2 symmetry consists of a single baryon (Λ^*) which has isospin $I = 0$ and hypercharge $Y = 0$ (strangeness $\mathcal{S} = -1$). In Figures 2 and 3 I show the corresponding weight diagrams for the octet and decuplet baryons. The explicit form of the spin and flavor wave functions is given in Appendix A.

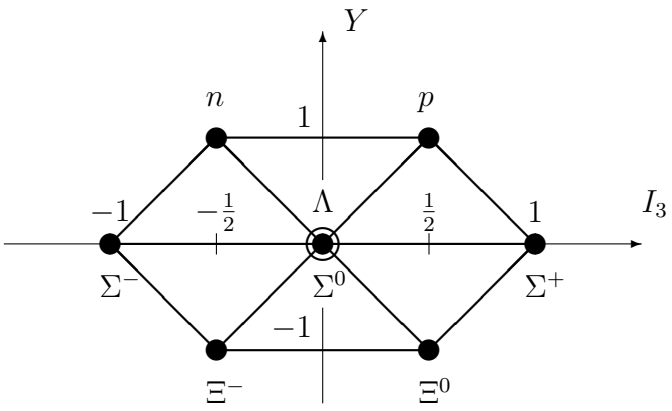

Figure 2: Baryon octet with $(p, q) = (1, 1)$ and $J^P = S^P = \frac{1}{2}^+$

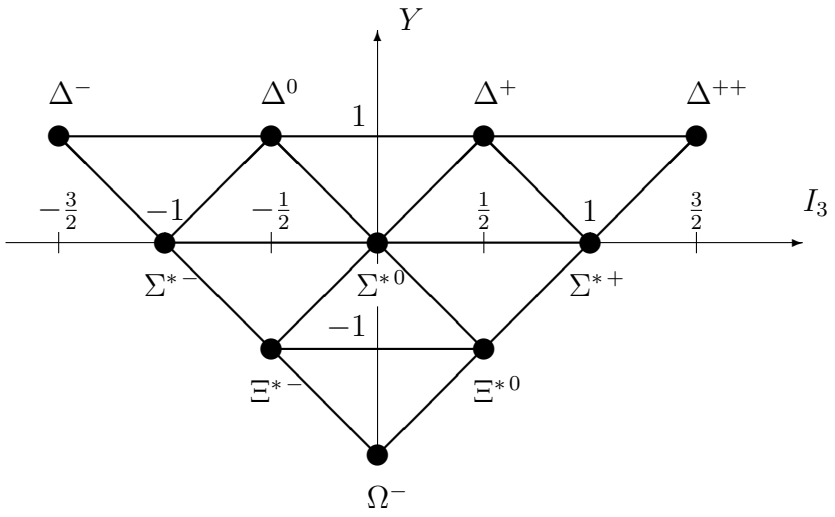

Figure 3: Baryon decuplet with $(p, q) = (3, 0)$ and $J^P = S^P = \frac{3}{2}^+$

2.2 $q\bar{q}$ Mesons

Just as for qqq baryons, the allowed spin and flavor states of $q\bar{q}$ mesons are obtained by standard group theoretic techniques [13, 14, 15]. The total spin of the quark-antiquark system is obtained by coupling the $\frac{1}{2}$ spins of the quark and antiquark to give $S = 0$ and $S = 1$. In the absence of orbital excitations the parity of the $q\bar{q}$ mesons is negative $P = -$. Therefore, the allowed values of the spin and parity of $q\bar{q}$ configurations are $J^P = S^P = 0^-$ (pseudoscalar mesons) and $J^P = S^P = 1^-$ (vector mesons).

The flavor states of the quark-antiquark system are obtained by taking the product

$$\begin{aligned} [1] \;\otimes\; [11] \;&=\; [21] \;\oplus\; [111] \\ \square \;\otimes\; \begin{array}{|c|}\hline\\\hline\end{array} \;&=\; \begin{array}{|c|c|}\hline\\\hline\end{array} \;\oplus\; \begin{array}{|c|}\hline\\\hline\\\hline\end{array} \end{aligned} \tag{2.9}$$

i.e. an octet [21] with $(p, q) = (1, 1)$ and a singlet [111] with $(p, q) = (0, 0)$. Finally, the spin-flavor states are denoted by their dimensions as [35] and [1], respectively. The allowed spin, flavor and spin-flavor states of $q\bar{q}$ mesons are summarized in Table 4.

The spin and flavor content of each spin-flavor multiplet is given by the decomposition of the representations of $SU_{\rm sf}(6)$ into those of $SU_{\rm f}(3) \otimes SU_{\rm s}(2)$

$$\begin{aligned} [35] \;&\supset\; {}^3 8 \,\oplus\, {}^3 1 \,\oplus\, {}^1 8 \,, \\ [1] \;&\supset\; {}^1 1 \,, \end{aligned} \tag{2.10}$$

where the superscript denotes $2S + 1$. The representation [35] contains the octet and singlet vector mesons with $S^P = 1^-$ as well as the octet of pseudoscalar mesons with $S^P = 0^-$, whereas the [1] representation only contains the singlet pseudoscalar meson with $S^P = 0^-$.

Table 4: Allowed color, spin, flavor and spin-flavor meson states

	$q\bar{q}$	Dimension
color	[111]	singlet
spin	[2]	3
	[11]	1
flavor	[21]	octet
	[111]	singlet
spin-flavor	[21111]	35
	[111111]	1

Table 5: Classification of ground state mesons according to $SU_{\rm f}(3) \supset SU_{\rm I}(2) \otimes U_{\rm Y}(1)$

			I	Y	Q
$J^P = 0^-$ octet	Kaon	K	$\frac{1}{2}$	1	0,1
	Pion	π	1	0	–1,0,1
	Eta	η_8	0	0	0
	Anti-kaon	$\overline{K}$	$\frac{1}{2}$	–1	–1,0
$J^P = 0^-$ singlet	Eta	η_1	0	0	0
$J^P = 1^-$ octet	Kaon	K^*	$\frac{1}{2}$	1	0,1
	Rho	ρ	1	0	–1,0,1
	Omega	ω_8	0	0	0
	Anti-kaon	$\overline{K}^*$	$\frac{1}{2}$	–1	–1,0
$J^P = 1^-$ singlet	Omega	ω_1	0	0	0

In Table 5 I present the classification of the pseudoscalar and vector meson octet in terms of the isospin I and the hypercharge Y according to the decomposition of the flavor symmetry $SU_{\rm f}(3)$ into $SU_{\rm I}(2) \otimes U_{\rm Y}(1)$. The kaons K and K^* carry strangeness $\mathcal{S} = +1$, and the antikaons $\overline{K}$ and $\overline{K}^*$ have strangeness $\mathcal{S} = -1$. The remaining mesons have strangeness $\mathcal{S} = 0$. In Figures 4 and 5 I show the corresponding weight diagrams for the pseudoscalar and vector meson octets. The explicit form of the spin and flavor wave functions is given in Appendix B.

The physical pseudoscalar mesons η and η' correspond to a mixture of the octet and singlet mesons

$$\begin{aligned} \eta(548) &= \eta_8 \cos\theta_P - \eta_1 \sin\theta_P \ , \\ \eta'(958) &= \eta_8 \sin\theta_P + \eta_1 \cos\theta_P \ , \end{aligned} \tag{2.11}$$

with a mixing angle $-20^\circ < \theta_P < -10^\circ$. For the vector mesons occurs something similar,

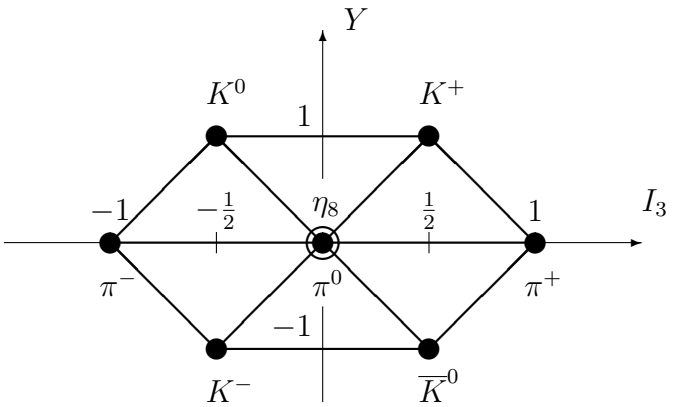

Figure 4: Pseudoscalar meson octet with $J^P = S^P = 0^-$

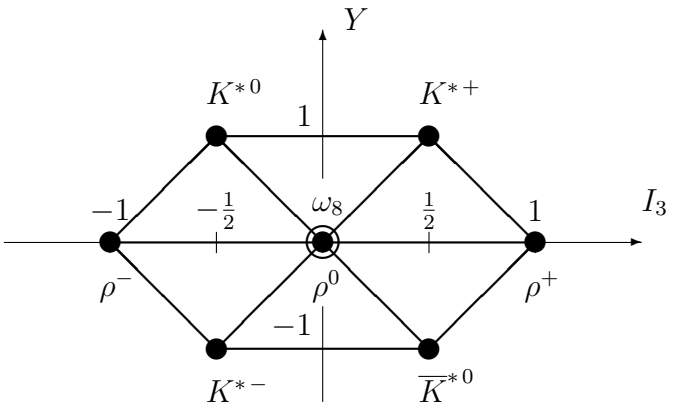

Figure 5: Vector meson octet with $J^P = S^P = 1^-$

the physical vector mesons ϕ and ω correspond to a mixture of the octet and singlet mesons

$$\begin{aligned} \phi(1020) &= \omega_8 \cos\theta_V - \omega_1 \sin\theta_V \ , \\ \omega(782) &= \omega_8 \sin\theta_V + \omega_1 \cos\theta_V \ , \end{aligned} \tag{2.12}$$

with a mixing angle $\theta_V \simeq 35^\circ$.

3 Quark models of baryons

One of the main goals of hadronic physics is to understand the structure of the nucleon and its excited states in terms of effective degrees of freedom and, at a more fundamental level, the emergence of these effective degrees of freedom from QCD, the underlying theory of quarks and gluons [16]. Despite the progress made in lattice calculations, it remains a daunting problem to solve the QCD equations in the non-perturbative region. Therefore,

one has developed effective models of hadrons, such as bag models, chiral quark models, soliton models [17], instanton liquid model [18] and the constituent quark model. Each of these approaches is constructed in order to mimic some selected properties of the strong interaction, but obviously none of them is QCD.

An important class is provided by constituent quark models (CQM) which are based on constituent (effective) quark degrees of freedoms. There exists a large variety of CQMs, among others the Isgur-Karl model [19], the Capstick-Isgur model [20], the collective model [21, 22], the hypercentral model [23], the chiral boson-exchange model [24] and the Bonn instanton model [25]. While these models display important and peculiar differences, they share the main features: the effective degrees of freedom of three constituent quarks (qqq configurations), the $SU(6)$ spin-flavor symmetry and a long-range confining potential. Each of these models reproduce the mass spectrum of baryon resonances reasonably well, but at the same time, they show very similar deviations for other observables, such as photocouplings, helicity amplitudes and strong decays (for a review, see Ref. [26]).

In this section, I review the so-called algebraic models of baryons with particular emphasis on the stringlike collective model [21, 22].

3.1 Algebraic models

The relative motion of the three constituent parts can be described in terms of Jacobi coordinates, $\vec{\rho}$ and $\vec{\lambda}$, which in the case of three identical objects are

$$\begin{aligned} \vec{\rho} &= \frac{1}{\sqrt{2}}(\vec{r}_1 - \vec{r}_2) \ , \\ \vec{\lambda} &= \frac{1}{\sqrt{6}}(\vec{r}_1 + \vec{r}_2 - 2\vec{r}_3) \ , \end{aligned} \tag{3.1}$$

where $\vec{r}_1$, $\vec{r}_2$ and $\vec{r}_3$ denote the end points of the string configuration in Figure 6. The method of bosonic quantization [21] consists in introducing a dipole boson $b_i^\dagger$ with $L^P = 1^-$ for each independent relative coordinate and its conjugate momentum, and adding an auxiliary scalar boson $s^\dagger$ with $L^P = 0^+$

$$s^\dagger \ , \ b^\dagger_{\rho,m} \ , \ b^\dagger_{\lambda,m} \ , \quad (m = 0, \pm 1) \ . \tag{3.2}$$

The scalar boson does not represent an independent degree of freedom, but is added under the restriction that the total number of bosons

$$\hat{N} \ = \ s^\dagger s + \sum_m \left(b^\dagger_{\rho,m} b_{\rho,m} + b^\dagger_{\lambda,m} b_{\lambda,m} \right) \ , \tag{3.3}$$

is conserved. This procedure leads to a compact spectrum generating algebra for the radial (or orbital) excitations

$$\mathcal{G}_{\rm orb} \ = \ U(7) \ , \tag{3.4}$$

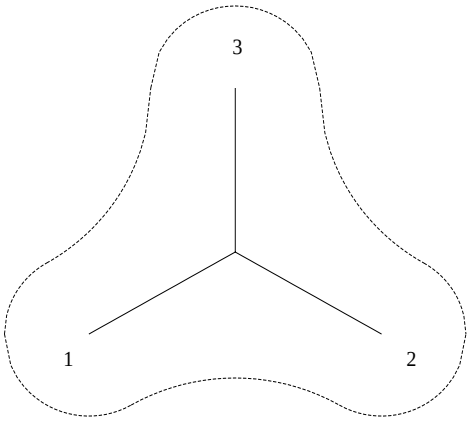

Figure 6: Collective model of baryons

which describes the transformations among the seven bosons of Eq. (3.2). For a system of interacting bosons the model space is spanned by the symmetric irreducible representation $[N]$ of $U(7)$. The value of N determines the size of the model space.

The S_3 permutation symmetry poses an additional constraint on the allowed interaction terms. The scalar boson, $s^\dagger$, transforms as the symmetric representation, A_1, while the two vector bosons, $b^\dagger_\rho$ and $b^\dagger_\lambda$, transform as the two components E_ρ and E_λ of the mixed symmetry representation E. The choice of the Jacobi coordinates in Eq. (3.1) is consistent with the conventions used for the spin and flavor wave functions used in the appendices. The eigenvalues and corresponding eigenvectors can be obtained exactly by diagonalization in an appropriate basis. The radial wave functions have, by construction, good angular momentum L, parity P, and permutation symmetry $t = A_1,\ E,\ A_2$. Moreover, the total number of bosons N is conserved.

The mass operator depends both on the spatial and the internal degrees of freedom. Whereas in nonrelativistic problems the spectrum is obtained by expanding the Hamiltonian in terms of the generators of the algebra $\mathcal{G}_{\rm orb}$, in algebraic models of hadrons one uses the mass-squared operator [21, 22]. In this section I discuss the contribution from the spatial part. The most general form of the radial part of the mass operator, that preserves angular momentum, parity and the total number of bosons, transforms as a scalar under the permutation group and is at most two-body in the boson operators, can be written as

$$\begin{aligned}
\hat{M}^2_{\rm orb} &= \epsilon_s\, s^\dagger \tilde{s} - \epsilon_p\, (b^\dagger_\rho \cdot \tilde{b}_\rho + b^\dagger_\lambda \cdot \tilde{b}_\lambda) + u_0\, (s^\dagger s^\dagger \tilde{s}\tilde{s}) - u_1\, s^\dagger (b^\dagger_\rho \cdot \tilde{b}_\rho + b^\dagger_\lambda \cdot \tilde{b}_\lambda)\tilde{s} \\
&+ v_0\, \left[(b^\dagger_\rho \cdot b^\dagger_\rho + b^\dagger_\lambda \cdot b^\dagger_\lambda)\tilde{s}\tilde{s} + s^\dagger s^\dagger (\tilde{b}_\rho \cdot \tilde{b}_\rho + \tilde{b}_\lambda \cdot \tilde{b}_\lambda) \right] \\
&+ \sum_{l=0,2} c_l\, \left[(b^\dagger_\rho \times b^\dagger_\rho - b^\dagger_\lambda \times b^\dagger_\lambda)^{(l)} \cdot (\tilde{b}_\rho \times \tilde{b}_\rho - \tilde{b}_\lambda \times \tilde{b}_\lambda)^{(l)} + 4\, (b^\dagger_\rho \times b^\dagger_\lambda)^{(l)} \cdot (\tilde{b}_\lambda \times \tilde{b}_\rho)^{(l)} \right] \\
&+ c_1\, (b^\dagger_\rho \times b^\dagger_\lambda)^{(1)} \cdot (\tilde{b}_\lambda \times \tilde{b}_\rho)^{(1)} + \sum_{l=0,2} w_l\, (b^\dagger_\rho \times b^\dagger_\rho + b^\dagger_\lambda \times b^\dagger_\lambda)^{(l)} \cdot (\tilde{b}_\rho \times \tilde{b}_\rho + \tilde{b}_\lambda \times \tilde{b}_\lambda)^{(l)}\ ,
\end{aligned} \tag{3.5}$$

with $\tilde{s} = s$ and $\tilde{b}_{i,m} = (-1)^{1-m} b_{i,-m}$. Here the dots indicate scalar products and the crosses tensor products with respect to the rotation group. The eigenvalues and corresponding eigenvectors of the mass-squared operator of Eq. (3.5) can be obtained exactly by numerical diagonalization. The wave functions obtained in this way have by construction good angular momentum, parity and permutation symmetry. The procedure to determine the permutation symmetry of a given wave function is described in [21, 22].

The mass-squared operator of Eq. (3.5) contains several models of baryon structure which arise for special choices of the coefficients. In the next sections two special solutions are discussed: the harmonic oscillator quark model and a stringlike collective model.

3.2 Harmonic oscillator quark model

Harmonic oscillator quark models correspond to the choice $v_0 = 0$, *i.e.* no coupling between different harmonic oscillator shells. The one-body terms of the S_3 invariant mass operator of Eq. (3.5) correspond to a harmonic oscillator

$$\hat{M}^2_{\rm orb} \;=\; \epsilon \sum_m \left(b^\dagger_{\rho,m} b_{\rho,m} + b^\dagger_{\lambda,m} b_{\lambda,m} \right) \;, \tag{3.6}$$

whereas the two-body interactions give rise to anharmonic contributions. The nonrelativistic harmonic oscillator quark model [19] is a model of this type, although it is written for the mass $\hat{M}$ rather than for $\hat{M}^2$. The equality of the frequencies of the ρ and λ oscillators is a consequence of the S_3 permutation symmetry. The mass spectrum is that of a six-dimensional harmonic oscillator

$$M^2_{\rm orb} \;=\; \epsilon \, (n_\rho + n_\lambda) \;, \tag{3.7}$$

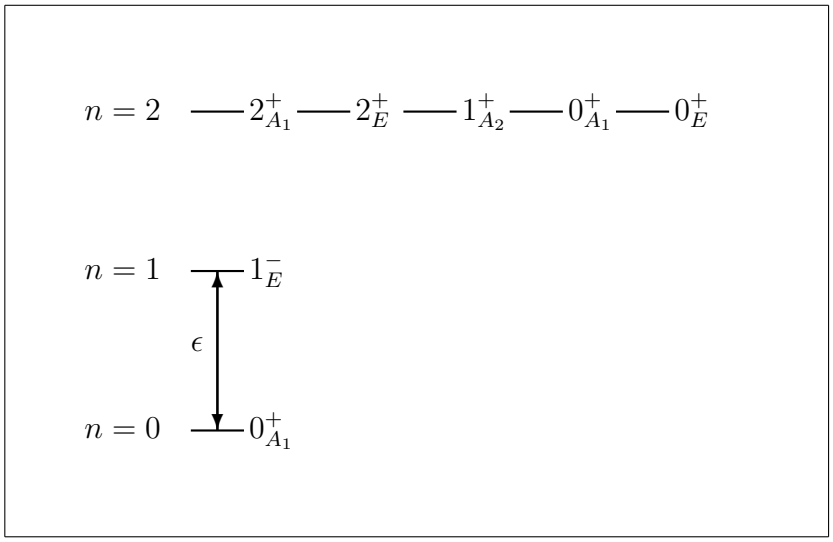

Figure 7: Schematic representation of the radial excitations of q^3 baryons in a harmonic oscillator model. The number of bosons is $N = 2$.

where $n_\rho + n_\lambda = n$ is the number of oscillator quanta. The model space consists of the oscillator shells with $n = 0, 1, \ldots, N$.

The mass spectrum for the harmonic oscillator is shown in Figure 7 for $N = 2$ bosons. The levels are grouped into oscillator shells characterized by n. The ground state has $n = 0$ and $L_t^P = 0_{A_1}^+$. The one-phonon multiplet $n = 1$ has two degenerate states with $L^P = 1^-$ which belong to the two-dimensional representation E, and the two-phonon multiplet $n = 2$ consists of the states $L_t^P = 2_{A_1}^+$, 2_E^+, $1_{A_2}^+$, $0_{A_1}^+$ and 0_E^+. The degenerate levels in an oscillator shell can be separated by introducing higher-order interactions in the mass operator.

3.3 Stringlike collective model

In the stringlike collective model the baryons are interpreted as rotational and vibrational excitations of the string configuration of Figure 6. The three constituent parts move in a correlated way. For three identical constituents the vibrations are described by [21, 22]

$$\begin{aligned} \hat{M}^2_{\rm vib} &= \xi_1 \left(R^2\, s^\dagger s^\dagger - b^\dagger_\rho \cdot b^\dagger_\rho - b^\dagger_\lambda \cdot b^\dagger_\lambda \right) \left(R^2\, \tilde{s}\tilde{s} - \tilde{b}_\rho \cdot \tilde{b}_\rho - \tilde{b}_\lambda \cdot \tilde{b}_\lambda \right) \\ &\quad + \xi_2 \left[\left(b^\dagger_\rho \cdot b^\dagger_\rho - b^\dagger_\lambda \cdot b^\dagger_\lambda \right) \left(\tilde{b}_\rho \cdot \tilde{b}_\rho - \tilde{b}_\lambda \cdot \tilde{b}_\lambda \right) + 4 \left(b^\dagger_\rho \cdot b^\dagger_\lambda \right) \left(\tilde{b}_\lambda \cdot \tilde{b}_\rho \right) \right] . \end{aligned} \tag{3.8}$$

The parameters ξ_1 and ξ_2 in Eq. (3.8) are linear combinations of those in Eq. (3.5). In particular, since now $v_0 = -\xi_1 R^2 \neq 0$, the corresponding eigenfunctions are collective in the sense that they are spread over many different oscillator shells.

Although the mass spectrum and corresponding eigenfunctions of $\hat{M}^2$ can be obtained numerically by diagonalization, approximate solutions exist in the limit of a large model space ($N \to \infty$) which can be used to gain insight into its physical content. In the large N limit the mass operator of Eq. (3.8) reduces to leading order in N to a harmonic form, and its eigenvalues are given by [21, 22]

$$M^2_{\rm vib} = \kappa_1\, v_1 + \kappa_2 \left(v_{2a} + v_{2b} \right) , \tag{3.9}$$

with

$$\kappa_1 = 4N\xi_1\, R^2 , \qquad \kappa_2 = 4N\xi_2\, R^2/(1+R^2) . \tag{3.10}$$

The vibrational mass operator of Eq. (3.8) has a very simple physical interpretation. Its spectrum has three fundamental vibrations (see Figure 8). The v_1-vibration is the symmetric stretching vibration along the direction of the strings (breathing mode), while the v_{2a}- and the v_{2b}-vibrations denote bending vibrations. The latter two are degenerate in the case of three identical objects. QCD-based arguments suggest that while the string is soft towards stretching, it is hard towards bending and thus one expects the v_2-vibration to lie higher than the v_1-vibration. The spectrum consists of a series of vibrational excitations characterized by the labels $(v_1, v_2) = (v_1, v_{2a} + v_{2b})$ and a tower of rotational excitations built on top of each vibration. The rotational states for each type of vibration are those of an oblate symmetric top.

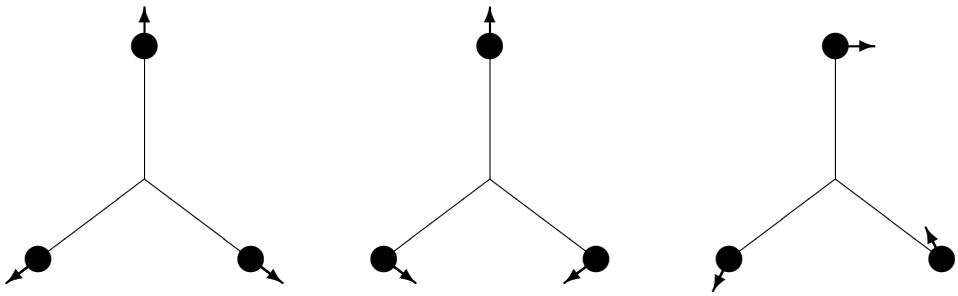

Figure 8: Vibrations of the string-like configuration of Figure 6

The occurrence of linear Regge trajectories suggests, that one should add a term linear in L to the mass operator

$$M^2_{\rm orb} \;=\; \kappa_1\, v_1 + \kappa_2\, v_2 + \alpha\, L\ . \tag{3.11}$$

A schematic spectrum of the stringlike collective model is presented in Figure 9. A comparison with the mass spectrum of Figure 7 shows that whereas for the harmonic oscillator the excited $L^\pi = 0^+$ states belong to the two-phonon ($n = 2$) multiplet, in the stringlike model they correspond to one-phonon vibrational excitations and are the

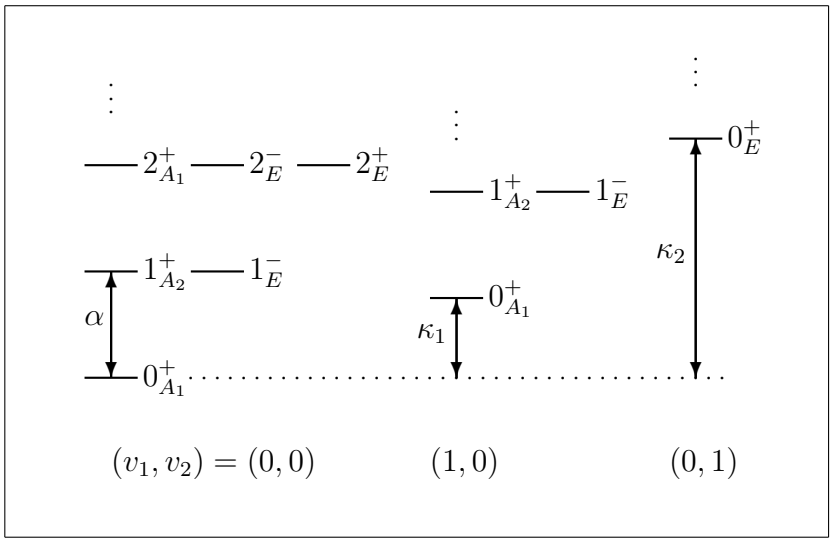

Figure 9: Schematic representation of the radial excitations of q^3 baryons in a stringlike collective model. The masses are calculated using Eq. (3.11) with $\kappa_1 > 0$, $\kappa_2 > 0$ and $\alpha > 0$.

bandheads of these fundamental vibrations.

3.4 Wave functions

The full algebraic structure is obtained by combining the spatial part $\mathcal{G}_{\rm orb}$ of Eq. (3.4) with the internal spin-flavor-color part $\mathcal{G}_{\rm sfc}$ of Eq. (2.1)

$$\mathcal{G} \;=\; \mathcal{G}_{\rm orb} \otimes \mathcal{G}_{\rm sfc} \;=\; U(7) \otimes SU_{\rm sf}(6) \otimes SU_{\rm c}(3) \;. \tag{3.12}$$

The baryon wave function is obtained by combining the spin-flavor part with the color and orbital parts in such a way that the total wave function is a color-singlet, and that the three quarks satisfy the Pauli principle, *i.e.* are antisymmetric under any permutation of the three quarks. Since the color-singlet part of the baryon wave function is antisymmetric ($t = A_2$, see Table 2), the orbital-spin-flavor part has to be symmetric ($t = A_1$)

$$\psi_{A_2} \;=\; \left[\psi^{\rm c}_{A_2} \times \psi^{\rm osf}_{A_1}\right]_{A_2} \;, \tag{3.13}$$

which means that the permutation symmetry of the spatial wave function is the same as that of the spin-flavor part (see Table 6)

$$\psi^{\rm osf}_{A_1} \;=\; \left[\psi^{\rm o}_{t} \times \psi^{\rm sf}_{t}\right]_{A_1} \;, \tag{3.14}$$

with $t = A_1$, E, A_2. The square brackets $[\cdots]$ denote the tensor coupling under the point group D_3.

In the more conventional notation, the total baryon wave function is expressed as

$$|\Psi\rangle \;=\; \left|\,^{2S+1}\dim\{SU_{\rm f}(3)\}_J\,[\dim\{SU_{\rm sf}(6)\}, L^P]\,\right\rangle \;, \tag{3.15}$$

where L, S and J are the orbital angular momentum, the spin and the total angular momentum $\vec{J} = \vec{L} + \vec{S}$. As an example, the wave function of the nucleon is given by

$$|\Psi_N\rangle \;=\; \left|N :\, ^2 8_{1/2}\,[56, 0^+]\,\right\rangle \;, \tag{3.16}$$

and that of the Δ resonance by

$$|\Psi_\Delta\rangle \;=\; \left|\Delta :\, ^4 10_{3/2}\,[56, 0^+]\,\right\rangle \;. \tag{3.17}$$

In Appendix C I present the space-spin-flavor baryon wave functions with S_3 symmetry.

Table 6: Discrete symmetry of q^3 baryon states

ψ	$\psi^{\rm c}$	$\psi^{\rm osf}$	$\psi^{\rm o}$	$\psi^{\rm sf}$
A_2	A_2	A_1	A_1	A_1
			E	E
			A_2	A_2

3.5 Mass spectrum

The mass spectrum of the baryon resonances is characterized by the lowlying N(1440) resonance with $J^P = 1/2^+$ (the socalled Roper resonance), whose mass is smaller than that of the first excited negative parity resonances, and the occurrence of linear Regge trajectories. The Roper resonance has the same quantum numbers as the nucleon of Eq. (3.16), but is associated with the first excited $L_t^P = 0_{A_1}^+$ state. In the harmonic oscillator the first excited $L_t^P = 0_{A_1}^+$ state belongs to the $n = 2$ positive parity multiplet which lies above the first excited negative parity state with $n = 1$ (see Figure 7), whereas the data show the opposite. In the stringlike collective model, the Roper resonance is a vibrational excitation whose mass is independent of that of the negative parity states which are interpreted as rotational excitations.

Furthermore, the data show that the mass-squared of the resonances depends linearly on the orbital angular momentum $M^2 \propto L$. The resonances belonging to such a Regge trajectory have the same quantum numbers with the exception of L. The trajectories for

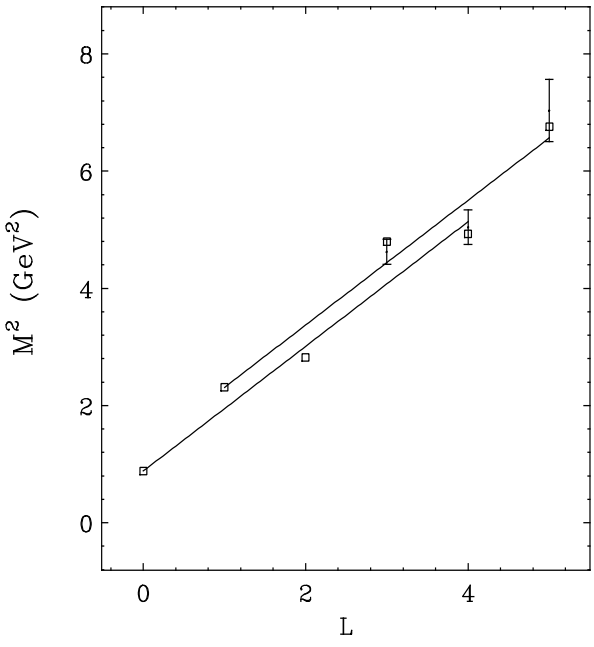

Figure 10: Regge trajectories for the positive parity resonances $|^2 8_{J=L+1/2}\,[56, L^+]\rangle$ with $L = 0, 2, 4$ and the negative parity resonances $|^2 8_{J=L+1/2}\,[70, L^-]\rangle$ with $L = 1, 3, 5$. The lines represent the result for the stringlike collective model.

Table 7: Values of the parameters in the mass formula of Eqs. (3.18) and (3.19) in GeV^2

Parameter	Ref. [22]
κ_1	1.204
κ_2	1.460
α	1.068
a	–0.041
b	0.017
c	0.130
d	–0.449
e	0.016
f	0.042
δ(MeV)	33

the positive parity resonances $|^2 8_{J=L+1/2}\,[56, L^+]\rangle$ with $L = 0, 2, 4$ and for the negative parity resonances $|^2 8_{J=L+1/2}\,[70, L^-]\rangle$ with $L = 1, 3, 5$ are shown in Figure 10. The slope of the Regge trajectories is almost the same for baryons $\alpha_B = 1.068$ (GeV)^2 [21] and for mesons $\alpha_M = 1.092$ (GeV)^2 [27]. Such a behavior is also expected on basis of soft QCD strings in which the strings elongate as they rotate [28]. The splitting of the rotational states in the harmonic oscillator is hard to reconcile with linear Regge trajectories.

In the stringlike collective model it is straightforward to reproduce the relative mass of the Roper resonance and the occurrence of linear Regge trajectories. The experimental mass spectrum of baryon resonances is analyzed in terms of the mass formula

$$M^2 \;=\; M_0^2 + M_{\rm orb}^2 + M_{\rm sf}^2 \;, \tag{3.18}$$

where the orbital part is taken from Eq. (3.11) and the spin-flavor part is expressed in a Gürsey-Radicati form [29], *i.e.* in terms of Casimir invariants of the spin-flavor group $SU_{\rm sf}(6)$ and its subgroups [22]

$$M_{\rm sf}^2 \;=\; a\,\left\langle C_{2SU_{\rm sf}(6)}\right\rangle + b\,\left\langle C_{2SU_{\rm f}(3)}\right\rangle + c\,S(S+1) + d\,Y + e\,Y^2 + f\,I(I+1)\;. \tag{3.19}$$

The explicit expressions of the eigenvalues of the Casimir operators of the spin-flavor and flavor groups can be found in [22]. The coefficient M_0^2 is determined by the nucleon mass. The remaining nine coefficients are obtained in a simultaneous fit to the 48 three and four star resonances which have been assigned as octet and decuplet states. A good overall fit is found with an r.m.s. deviation of $\delta = 33$ MeV. The values of the parameters are given in Table 7.

Tables 8 and 9 and show that the mass formula of Eqs. (3.18,3.19) provides a good overall description of both positive and negative baryon resonances belonging to the N, Δ, Σ, Λ, Ξ and Ω families. There is no need for an additional energy shift for the positive parity states and another one for the negative parity states, as in the relativized quark model [20].

Table 8: Mass spectrum of nonstrange baryon resonances in the stringlike (oblate top) model. The masses are given in MeV. The experimental values are taken from [2].

Baryon $L_{2I,2J}$	Status	Mass	State	(v_1, v_2)	$M_{\rm calc}$
$N(939)P_{11}$	****	939	${}^2 8_{1/2}[56, 0^+]$	(0,0)	939
$N(1440)P_{11}$	****	1430-1470	${}^2 8_{1/2}[56, 0^+]$	(1,0)	1444
$N(1520)D_{13}$	****	1515-1530	${}^2 8_{3/2}[70, 1^-]$	(0,0)	1563
$N(1535)S_{11}$	****	1520-1555	${}^2 8_{1/2}[70, 1^-]$	(0,0)	1563
$N(1650)S_{11}$	****	1640-1680	${}^4 8_{1/2}[70, 1^-]$	(0,0)	1683
$N(1675)D_{15}$	****	1670-1685	${}^4 8_{5/2}[70, 1^-]$	(0,0)	1683
$N(1680)F_{15}$	****	1675-1690	${}^2 8_{5/2}[56, 2^+]$	(0,0)	1737
$N(1700)D_{13}$	***	1650-1750	${}^4 8_{3/2}[70, 1^-]$	(0,0)	1683
$N(1710)P_{11}$	***	1680-1740	${}^2 8_{1/2}[70, 0^+]$	(0,1)	1683
$N(1720)P_{13}$	****	1650-1750	${}^2 8_{3/2}[56, 2^+]$	(0,0)	1737
$N(2190)G_{17}$	****	2100-2200	${}^2 8_{7/2}[70, 3^-]$	(0,0)	2140
$N(2220)H_{19}$	****	2180-2310	${}^2 8_{9/2}[56, 4^+]$	(0,0)	2271
$N(2250)G_{19}$	****	2170-2310	${}^4 8_{9/2}[70, 3^-]$	(0,0)	2229
$N(2600)I_{1,11}$	***	2550-2750	${}^2 8_{11/2}[70, 5^-]$	(0,0)	2591
$\Delta(1232)P_{33}$	****	1230-1234	${}^4 10_{3/2}[56, 0^+]$	(0,0)	1246
$\Delta(1600)P_{33}$	***	1550-1700	${}^4 10_{3/2}[56, 0^+]$	(1,0)	1660
$\Delta(1620)S_{31}$	****	1615-1675	${}^2 10_{1/2}[70, 1^-]$	(0,0)	1649
$\Delta(1700)D_{33}$	****	1670-1770	${}^2 10_{3/2}[70, 1^-]$	(0,0)	1649
$\Delta(1905)F_{35}$	****	1870-1920	${}^4 10_{5/2}[56, 2^+]$	(0,0)	1921
$\Delta(1910)P_{31}$	****	1870-1920	${}^4 10_{1/2}[56, 2^+]$	(0,0)	1921
$\Delta(1920)P_{33}$	***	1900-1970	${}^4 10_{3/2}[56, 2^+]$	(0,0)	1921
$\Delta(1930)D_{35}$	***	1920-1970	${}^2 10_{5/2}[70, 2^-]$	(0,0)	1946
$\Delta(1950)F_{37}$	****	1940-1960	${}^4 10_{7/2}[56, 2^+]$	(0,0)	1921
$\Delta(2420)H_{3,11}$	****	2300-2500	${}^4 10_{11/2}[56, 4^+]$	(0,0)	2414

In addition to the resonances presented in the tables, there are many more states calculated than have been observed so far, especially in the nucleon sector [22]. The lowest socalled 'missing' resonances correspond mostly to the unnatural parity states with $L^P = 1^+, 2^-$, which are decoupled both in electromagnetic and strong decays, and hence difficult to observe.

Whereas the spectrum of octet and decuplet resonances are described very well in the stringlike collective model, there are three states which show a deviation of about 100 MeV or more from the data: the $\Lambda^*(1405)$, $\Lambda^*(1520)$ and $\Lambda^*(2100)$ resonances are overpredicted by 236, 121 and 97 MeV, respectively. These three resonances are assigned as singlet states in Table 9 (and were not included in the fitting procedure). The mass splitting of 115 MeV between $\Lambda^*(1405)$ and $\Lambda^*(1520)$ can be obtained by including a spin-orbit interaction. However, in the rest of the baryon spectra there is no evidence

Table 9: As Table 8, but for strange baryon resonances. Note, that Ξ resonances are denoted by $L_{2I,2J}$.

Baryon $L_{I,2J}$	Status	Mass	State	(v_1, v_2)	$M_{\rm calc}$
$\Sigma(1193)P_{11}$	****	1193	$^2 8_{1/2}[56, 0^+]$	(0,0)	1170
$\Sigma(1660)P_{11}$	***	1630-1690	$^2 8_{1/2}[56, 0^+]$	(1,0)	1604
$\Sigma(1670)D_{13}$	****	1665-1685	$^2 8_{3/2}[70, 1^-]$	(0,0)	1711
$\Sigma(1750)S_{11}$	***	1730-1800	$^2 8_{1/2}[70, 1^-]$	(0,0)	1711
$\Sigma(1775)D_{15}$	****	1770-1780	$^4 8_{5/2}[70, 1^-]$	(0,0)	1822
$\Sigma(1915)F_{15}$	****	1900-1935	$^2 8_{5/2}[56, 2^+]$	(0,0)	1872
$\Sigma(1940)D_{13}$	***	1900-1950	$^2 8_{3/2}[56, 1^-]$	(0,1)	1974
$\Sigma^*(1385)P_{13}$	****	1383-1385	$^4 10_{3/2}[56, 0^+]$	(0,0)	1382
$\Sigma^*(2030)F_{17}$	****	2025-2040	$^4 10_{7/2}[56, 2^+]$	(0,0)	2012
$\Lambda(1116)P_{01}$	****	1116	$^2 8_{1/2}[56, 0^+]$	(0,0)	1133
$\Lambda(1600)P_{01}$	***	1560-1700	$^2 8_{1/2}[56, 0^+]$	(1,0)	1577
$\Lambda(1670)S_{01}$	****	1660-1680	$^2 8_{1/2}[70, 1^-]$	(0,0)	1686
$\Lambda(1690)D_{03}$	****	1685-1690	$^2 8_{3/2}[70, 1^-]$	(0,0)	1686
$\Lambda(1800)S_{01}$	***	1720-1850	$^4 8_{1/2}[70, 1^-]$	(0,0)	1799
$\Lambda(1810)P_{01}$	***	1750-1850	$^2 8_{1/2}[70, 0^+]$	(0,1)	1799
$\Lambda(1820)F_{05}$	****	1815-1825	$^2 8_{5/2}[56, 2^+]$	(0,0)	1849
$\Lambda(1830)D_{05}$	****	1810-1830	$^4 8_{5/2}[70, 1^-]$	(0,0)	1799
$\Lambda(1890)P_{03}$	****	1850-1910	$^2 8_{3/2}[56, 2^+]$	(0,0)	1849
$\Lambda(2110)F_{05}$	****	2090-2140	$^4 8_{5/2}[70, 2^+]$	(0,0)	2074
$\Lambda(2350)H_{09}$	***	2340-2370	$^2 8_{9/2}[56, 4^+]$	(0,0)	2357
$\Lambda^*(1405)S_{01}$	****	1402-1410	$^2 1_{1/2}[70, 1^-]$	(0,0)	1641
$\Lambda^*(1520)D_{03}$	****	1518-1520	$^2 1_{3/2}[70, 1^-]$	(0,0)	1641
$\Lambda^*(2100)G_{07}$	****	2090-2110	$^2 1_{7/2}[70, 3^-]$	(0,0)	2197
$\Xi(1318)P_{11}$	****	1314-1316	$^2 8_{1/2}[56, 0^+]$	(0,0)	1334
$\Xi(1820)D_{13}$	***	1818-1828	$^2 8_{3/2}[70, 1^-]$	(0,0)	1828
$\Xi^*(1530)P_{13}$	****	1531-1532	$^4 10_{3/2}[56, 0^+]$	(0,0)	1524
$\Omega(1672)P_{03}$	****	1672-1673	$^4 10_{3/2}[56, 0^+]$	(0,0)	1670

for such a large spin-orbit coupling. This problem is common to qqq models of baryons (*e.g.* the constituent quark model with chromodynamics, either in its nonrelativistic [19] or its relativized form [20], and the chiral constituent quark model [30] all overpredict the $\Lambda^*(1405)$ mass). Another explanation for the mass splitting between $\Lambda^*(1520)$ and $\Lambda^*(1405)$ is the proximity of the $\Lambda^*(1405)$ resonance to the $N\overline{K}$ threshold. The inclusion of the coupling to the $N\overline{K}$ and $\Sigma\pi$ decay channels produces a downward shift of the qqq state toward or even below the $N\overline{K}$ threshold [31]. Such an interpretation is supported by the strong and electromagnetic couplings [22, 32, 33]. In a chiral meson-baryon Lagrangian approach with an effective coupled-channel potential the $\Lambda^*(1405)$ resonance emerges as a quasi-bound state of $N\overline{K}$ [34].

3.6 Magnetic moments

The magnetic moment of a multiquark system is given by the sum of the magnetic moments of its constituent parts

$$\vec{\mu} \;=\; \vec{\mu}_{\rm spin} + \vec{\mu}_{\rm orb} \;=\; \sum_i \mu_i (2\vec{s}_i + \vec{\ell}_i) \;, \tag{3.20}$$

where $\mu_i = e_i/2m_i$, e_i and m_i represent the magnetic moment, the electric charge and the mass of the i-th constituent.

The orbital-spin-flavor wave function of the ground state baryons is given by

$$\psi^{\rm osf}_{A_1} \;=\; \left[\psi^{\rm o}_{A_1} \times \psi^{sf}_{A_1}\right]_{A_1} \;. \tag{3.21}$$

The spin-flavor part can be expressed in terms of the flavor ϕ and spin χ wave function as

$$\psi^{\rm sf}_{A_1} \;=\; \left[\phi_{A_1} \times \chi_{A_1}\right]_{A_1} \;=\; \phi_{A_1}\chi_{A_1} \;, \tag{3.22}$$

for the decuplet baryons and

$$\psi^{\rm sf}_{A_1} \;=\; \left[\phi_E \times \chi_E\right]_{A_1} \;=\; \frac{1}{\sqrt{2}}\left(\phi_{E_\rho}\chi_{E_\rho} + \phi_{E_\lambda}\chi_{E_\lambda}\right) \;, \tag{3.23}$$

for the octet baryons. Since the orbital wave function of the ground state baryons has $L^P_t \;=\; 0^+_{A_1}$ (see Table 8), the magnetic moment only depends on the spin part. The magnetic moments of the Δ^{++} and the proton can be derived using the explicit expressions of the corresponding flavor and spin wave functions given in the appendices

$$\mu_{\Delta^{++}} \;=\; 3\mu_u \;, \qquad \mu_p \;=\; \frac{1}{3}(4\mu_u - \mu_d) \;. \tag{3.24}$$

Similarly, the magnetic moment of the neutron can be derived as

$$\mu_n \;=\; \frac{1}{3}(4\mu_d - \mu_u) \;. \tag{3.25}$$

Table 10: Magnetic moments of the ground state octet and decuplet baryons in μ_N. Experimental data are taken from [2].

	$\mu_{\rm th}$	$\mu_{\rm calc}$	$\mu_{\rm exp}$
p	$(4\mu_u - \mu_d)/3$	2.793	2.793
n	$(4\mu_d - \mu_u)/3$	-1.913	-1.913
Λ	μ_s	-0.613	-0.613 ± 0.004
Σ^+	$(4\mu_u - \mu_s)/3$	2.674	2.458 ± 0.010
Σ^0	$(2\mu_u + 2\mu_d - \mu_s)/3$	0.791	
Σ^-	$(4\mu_d - \mu_s)/3$	-1.092	-1.160 ± 0.025
Ξ^0	$(4\mu_s - \mu_u)/3$	-1.435	-1.250 ± 0.014
Ξ^-	$(4\mu_s - \mu_d)/3$	-0.493	-0.651 ± 0.003
Δ^{++}	$3\mu_u$	5.556	5.6 ± 1.9
Δ^+	$2\mu_u + \mu_d$	2.732	
Δ^0	$\mu_u + 2\mu_d$	-0.092	
Δ^-	$3\mu_d$	-2.916	
$\Sigma^{*,+}$	$2\mu_u + \mu_s$	3.091	
$\Sigma^{*,0}$	$\mu_u + \mu_d + \mu_s$	0.267	
$\Sigma^{*,-}$	$2\mu_d + \mu_s$	-2.557	
$\Xi^{*,0}$	$\mu_u + 2\mu_s$	0.626	
$\Xi^{*,-}$	$\mu_d + 2\mu_s$	-2.198	
Ω^-	$3\mu_s$	-1.839	-2.02 ± 0.05

In the limit of isospin symmetry $m_u = m_d$, one recovers the well-known relation for the magnetic moment ratio [35]

$$\frac{\mu_n}{\mu_p} \;=\; -\frac{2}{3}\;, \tag{3.26}$$

which is very close to the experimental value -0.685.

The magnetic moments of all ground state octet and decuplet baryons are given in Table 10. The quark magnetic moments μ_u, μ_d and μ_s are determined from the proton, neutron and Λ magnetic moments to be $\mu_u = 1.852\ \mu_N$, $\mu_d = -0.972\ \mu_N$ and $\mu_s = -0.613\ \mu_N$ [2]. The corresponding constituent quark masses are $m_u = 0.338$ GeV, $m_d = 0.322$ GeV, $m_s = 0.510$ GeV. Table 10 shows that the quark model results are in good agreement with the available experimental data.

The magnetic moments of decuplet baryons satisfy generalized Coleman-Glashow sum rules [36, 37]

$$\begin{aligned}
\mu_{\Delta^{++}} + \mu_{\Delta^-} &= \mu_{\Delta^+} + \mu_{\Delta^0}\;, \\
\mu_{\Delta^{++}} + \mu_{\Omega^-} &= \mu_{\Sigma^{*,+}} + \mu_{\Xi^{*,0}}\;, \\
\mu_{\Delta^-} + \mu_{\Omega^-} &= \mu_{\Sigma^{*,-}} + \mu_{\Xi^{*,-}}\;,
\end{aligned} \tag{3.27}$$

and

$$2\mu_{\Sigma^{*,0}} \;=\; \mu_{\Sigma^{*,-}} + \mu_{\Sigma^{*,+}} \;=\; \mu_{\Delta^+} + \mu_{\Xi^{*,-}} \;=\; \mu_{\Delta^0} + \mu_{\Xi^{*,0}} \;. \tag{3.28}$$

The same sum rules hold for the chiral quark-soliton model in the chiral limit [38].

In the limit of equal quark masses $m_u = m_d = m_s = m$, the magnetic moments of the decuplet pentaquark states become proportional to their electric charges [35]

$$\mu_i \;=\; \frac{e}{2m} Q_i \;, \tag{3.29}$$

which means that the sum of the magnetic moments of all members of the decuplet vanishes identically $\sum_i \mu_i = 0$.

3.7 Electromagnetic couplings

Electromagnetic couplings are of crucial importance in unraveling the structure of hadrons, since they are far more sensitive to wave functions (and models) than masses. It has become customary to characterize the transverse couplings by the helicity amplitudes, $A_{1/2}$ and $A_{3/2}$. These amplitudes are measurable in photo- and electroproduction. Their study is a major part of the experimental program at the new electron facilities [39].

Helicity amplitudes can be obtained by considering the nonrelativistic reduction of the coupling of the point-like constituents inside the baryon to the electromagnetic field [21]

$$\mathcal{H}_{\rm nr} \;=\; -\sum_{j=1}^{3} \left[\frac{e_j}{2m_j} (\vec{p}_j \cdot \vec{A}_j + \vec{A}_j \cdot \vec{p}_j) + 2\mu_j \vec{s}_j \cdot (\vec{\nabla} \times \vec{A}_j) \right] \;, \tag{3.30}$$

where m_j, e_j, $\vec{s}_j$ and $\mu_j = g e_j / 2m_j$ denote the mass, charge, spin and magnetic moment of the j–th constituent, respectively, and $\vec{A}_j \equiv \vec{A}(\vec{r}_j)$.

Details of the evaluation of helicity amplitudes in the stringlike collective models can be found in Refs. [21, 32]. As an example, the helicity amplitudes for the excitation of the $\Delta(1232)P_{33}$ resonance are given by

$$\begin{aligned} A_{1/2} \;&=\; -\frac{2\sqrt{2}}{3} \sqrt{\frac{\pi}{k_0}} \mu k \frac{1}{(1+k^2a^2)^2} \;, \\ A_{3/2} \;&=\; -\frac{2\sqrt{2}}{\sqrt{3}} \sqrt{\frac{\pi}{k_0}} \mu k \frac{1}{(1+k^2a^2)^2} \;. \end{aligned} \tag{3.31}$$

Their ratio $A_{3/2}/A_{1/2} = \sqrt{3}$ is independent of k and is in good agreement with the experimental value of the ratio for the photocouplings 1.85 ± 0.10 [2]. However, the absolute values are underpredicted by about 35 %. As another example we consider the helicity amplitudes of the $\mathrm{N}(1520)D_{13}$ resonance

$$\begin{aligned} A_{1/2} \;&=\; 2i \sqrt{\frac{\pi}{k_0}} \mu \frac{1}{(1+k^2a^2)^2} \Big[\frac{m_q k_0 a}{g} - k^2 a \Big] \;, \\ A_{3/2} \;&=\; 2i\sqrt{3} \sqrt{\frac{\pi}{k_0}} \mu \frac{1}{(1+k^2a^2)^2} \frac{m_q k_0 a}{g} \;. \end{aligned} \tag{3.32}$$

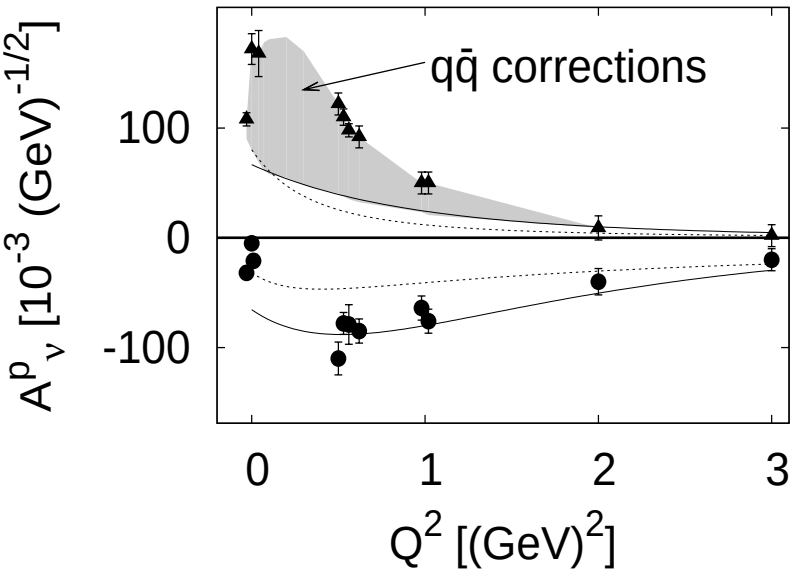

Figure 11: The helicity amplitudes as a function of Q^2 for the $D_{13}(1520)$ resonance. Experimental data [40] are compared with theoretical predictions from the collective $U(7)$ model [21, 32] (dotted line) and the hypercentral model [23] (solid line). The dashed line corresponds to a fit to the experimental data.

A comparison with the experimental data shows that the helicity amplitudes are underpredicted for small values of Q^2. This is a typical feature of quark models based on three valence quarks only. The problem of missing strength at low values of Q^2 can be attributed to the importance of quark-antiquark degrees of freedom, which become more important in the outer region of the nucleon.

4 The unquenched quark model for baryons

In the constituent quark model (CQM) hadrons are described in terms of system of constituent (or valence) quarks and antiquarks, qqq for baryons and $q\bar{q}$ for mesons. Despite the success of the quark model there is strong evidence for the existence of exotic degrees of freedom (other than valence quarks) in hadrons, Common features of constituent quark models are the effective degrees of freedom of three constituent quarks (qqq configurations), the $SU(6)$ spin-flavor symmetry and a long-range confining potential. Each of these models reproduce the mass spectrum of baryon resonances reasonably well, but at the same time, they show very similar deviations for other observables, such as photocouplings, helicity amplitudes and strong decays. Since the photocouplings depend mostly on the spin-flavor structure, all models that have the same $SU(6)$ structure in common, show the same behavior, *e.g.* the photocouplings for the $\Delta(1232)$ are underpredicted by a

large amount, even though their ratio is reproduced correctly. In general, the helicity amplitudes (or transition form factors) show deviations from CQM calculations at low values of Q^2 [41] (see Fig. 11 for the $D_{13}(1520)$ resonance). The problem of missing strength at low Q^2 indicates that some fundamental mechanism is lacking in the dynamical description of hadronic structure. This mechanism can be identified with the production of quark-antiquark pairs [42, 43], which becomes more important in the outer region of the nucleon.

Additional evidence for higher Fock components in the baryon wave function ($qqq - q\bar{q}$ configurations) comes from CQM studies of strong decay widths of baryon resonances that are on average underpredicted by CQMs [22, 33, 44], the spin-orbit splitting of $\Lambda(1405)$ and $\Lambda(1520)$, the low Q^2 behavior of transition form factors, and the large η decay widths of $N(1535)$, $\Lambda(1670)$ and $\Sigma(1750)$. More direct evidence for the importance of quark-antiquark components in the proton comes from measurements of the $\bar{d}/\bar{u}$ asymmetry in the nucleon sea [9, 10], the proton spin crisis [45, 46] and parity-violating electron scattering experiments which report a nonvanishing strange quark contribution, albeit small, to the charge and magnetization distributions [11, 12].

The role of higher Fock components in baryon wave functions has been studied by many authors in the context of meson cloud models, such as the cloudy bag model, meson convolution models and chiral models [9, 47]. In these models, the flavor asymmetry of the proton can be understood in terms of couplings to the pion cloud. There have also been several attempts to study the importance of higher Fock components in the context of the constituent quark model. In this respect we mention the work by Riska and coworkers who introduce a small number of selected higher Fock components which are then fitted to reproduce the experimental data [48]. However, these studies lack an explicit model or mechanism for the mixing between the valence and sea quarks. The Rome group studied the pion and nucleon electromagnetic form factors in a Bethe-Salpeter approach, mainly thanks to the dressing of photon vertex by means of a vector-meson dominance parametrization [49]. Koniuk and Guiasu used a convolution model with CQM wave functions and an elementary emission model for the coupling to the pion cloud to calculate the magnetic moments and the helicity amplitudes from the nucleon to the Δ resonance [50]. It was found that the nucleon magnetic moments were unchanged after renomalization of the parameters, but that the missing strength in the helicity amplitudes of the Δ could not be explained with pions only.

The impact of $q\bar{q}$ pairs in hadron spectroscopy was originally studied by Törnqvist and Zenczykowski in a quark model extended by the $^3P_0$ model [51]. Even though their model only includes a sum over ground state baryons and ground state mesons, the basic idea of the importance to carry out a sum over a complete set of intermediate states was proposed in there. Subsequently, the effects of hadron loops in mesons was studied by Geiger and Isgur in a flux-tube breaking model in which the $q\bar{q}$ pairs are created in the $^3P_0$ state with the quantum numbers of the vacuum [52, 53, 54]. In this approach, the quark potential model arises from an adiabatic approximation to the gluonic degrees of freedom embodied in the flux-tube [55]. It was shown that cancellations between apparently uncorrelated sets of intermediate states occur in such a way that the modification in the linear potential can

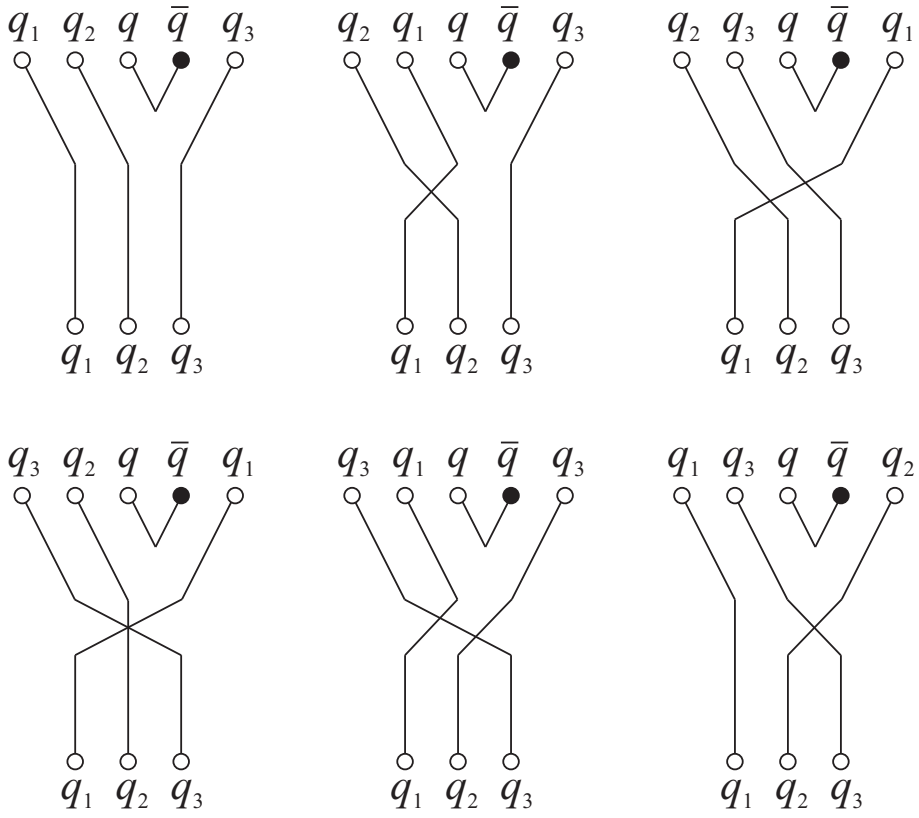

Figure 12: Quark line diagrams for $A \to BC$ with $q\bar{q} = s\bar{s}$ and $q_1q_2q_3 = uud$.

be reabsorbed, after renormalization, in the new strength of the linear potential [53]. In addition, the quark-antiquark pairs do not destroy the good CQM results for the mesons [53] and preserve the OZI hierarchy [54] provided that the sum be carried out over a large tower of intermediate states. A first application of this procedure to baryons was presented in [56] in which the importance of $s\bar{s}$ loops in the proton were studied by taking into account the contribution of the six diagrams of Fig. 12 in combination with harmonic oscillator wave functions for the baryons and mesons and a $^3P_0$ pair creation mechanism. This approach has the advantage that the effects of quark-antiquark pairs are introduced explicitly via a QCD-inspired pair-creation mechanism, which opens the possibility to study the importance of $q\bar{q}$ pairs in baryons and mesons in a systematic and unified way.

In this section, I present some recent work on the formulation of an unquenched quark model, which is part of a collaboration between groups from the University of Genova and UNAM, in which the effects of quark-antiquark pair creation ($u\bar{u}$, $d\bar{d}$ and $s\bar{s}$) are taken into account in an explicit form via a $^3P_0$ coupling mechanism [57, 58, 59]. In order to test the consistency of the formalism we first calculate the baryon magnetic moments [57] which constitute one of the early successes of the CQM. Finally, I discuss the spin and flavor content of the proton in the unquenched quark model. It is shown that the inclusion of hadron loops leads automatically to an excess of $\bar{d}$ over $\bar{u}$ and introduces a sizeable contribution of orbital angular momentum to the spin of the proton. Whereas the

flavor asymmetry and the orbital angular momentum are dominated by pion loops, the contribution of the sea quark spins to the proton spin arises almost entirely from (excited) vector meson loops. The numerical results for the flavor asymmetry [58] and the proton spin [57] are analyzed by means of a simple exactly solvable meson-cloud model [60].

4.1 Formalism

The impact of $q\bar{q}$ pairs in hadron spectroscopy was originally studied by Törnqvist and Zenczykowski in a quark model extended by the $^3P_0$ model [51]. Subsequently, the effects of hadron loops in mesons was studied by Geiger and Isgur in a flux-tube breaking model in which the $q\bar{q}$ pairs are created in the $^3P_0$ state with the quantum numbers of the vacuum [53, 54]. It was shown that cancellations between apparently uncorrelated sets of intermediate states occur in such a way that the modification in the linear potential can be reabsorbed, after renormalization, in the new strength of the linear potential [53]. In addition, the quark-antiquark pairs do not destroy the good CQM results for the mesons [53] and preserve the OZI hierarchy [54] provided that the sum be carried out over a large tower of intermediate states. The basic idea of the importance to carry out a sum over a complete set of intermediate states was already contained in [51]. An extension to baryons was presented in [56] in which the effects of $s\bar{s}$ loops in the proton were studied combining harmonic oscillator wave functions for baryons and mesons and a $^3P_0$ pair creation mechanism.

The present approach is motivated by earlier studies on extensions of the quark model that employ a $^3P_0$ model for the $q\bar{q}$ pair creation [51, 56]. Our approach is based on a CQM to which the quark-antiquark pairs with vacuum quantum numbers are added as a perturbation [56, 57, 58]. The pair-creation mechanism is inserted at the quark level and the one-loop diagrams are calculated by summing over a complete set of intermediate baryon-meson states (BC in Figure 13). Under these assumptions, the baryon wave function consists of a zeroth order three-quark configuration $\mid A\rangle$ plus a sum over all possible higher Fock components due to the creation of $^3P_0$ quark-antiquark pairs

$$\mid \psi_A\rangle \;=\; \mathcal{N}\left[\mid A\rangle + \sum_{BClJ}\int d\vec{k}\;\mid BC\vec{k}\,lJ\rangle\frac{\langle BC\vec{k}\,lJ\mid T^\dagger\mid A\rangle}{M_A-E_B-E_C}\right]\;. \tag{4.1}$$

Here A denotes the initial baryon, B and C represent the intermediate baryon and meson, and M_A, E_B and E_C are their respective energies, $\vec{k}$ and l the relative radial momentum and orbital angular momentum of B and C, and J is the total angular momentum $\vec{J}=\vec{J}_B+\vec{J}_C+\vec{l}$. The operator $T^\dagger$ creates a quark-antiquark pair in the $^3P_0$ state with the quantum numbers of the vacuum: $L=S=1$ and $J=0$ [57, 58, 61]

$$\begin{aligned} T^\dagger \;=\; -3\sum_{ij}\int d\vec{p}_i\,d\vec{p}_j\,\delta(\vec{p}_i+\vec{p}_j)\,C_{ij}\,F_{ij}\,\Gamma(\vec{p}_i-\vec{p}_j) \\ [\chi_{ij}\times\mathcal{Y}_1(\vec{p}_i-\vec{p}_j)]^{(0)}\,b_i^\dagger(\vec{p}_i)\,d_j^\dagger(\vec{p}_j)\;. \end{aligned} \tag{4.2}$$

Here, $b_i^\dagger(\vec{p}_i)$ and $d_j^\dagger(\vec{p}_j)$ are the creation operators for a quark and antiquark with momenta $\vec{p}_i$ and $\vec{p}_j$, respectively. The quark pair is characterized by a color singlet wave function

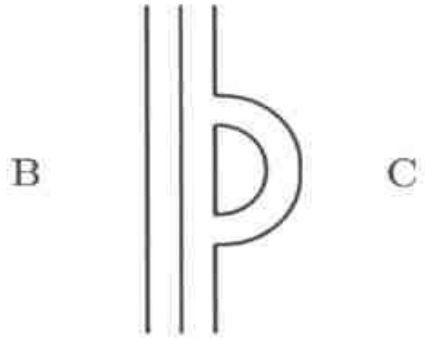

Figure 13: One-loop diagram at the quark level

C_{ij}, a flavor singlet wave function F_{ij} and a spin triplet wave function χ_{ij} with spin $S = 1$. The solid harmonic $\mathcal{Y}_1(\vec{p}_i - \vec{p}_j)$ indicates that the quark and antiquark are in a relative P wave. The $SU(3)$ flavor symmetry of the valence quark configuration $\mid A\rangle$ is broken by the quark-antiquark pairs via the energy denominator, but the $SU(2)$ isospin symmetry is still preserved. In the special case of the closure limit in which the energy denominator of Eq. (4.1) is a constant, the flavor symmetry of the valence quark configuration is recovered.

Since the operator $T^\dagger$ creates a pair of constituent quarks, a Gaussian quark-antiquark creation vertex function was introduced by which the pair is created as a finite object with an effective size, rather than as a pointlike object. In momentum space it is given by

$$\Gamma(\vec{p}_i - \vec{p}_j) \;=\; \gamma_0 \, \mathrm{e}^{-r_q^2 (\vec{p}_i - \vec{p}_j)^2/6} \; . \tag{4.3}$$

The width has been determined from meson decays to be approximately $0.25 - 0.35$ fm [54, 56, 62]. Here we take the average value, $r_q = 0.30$ fm. Finally, the dimensionless constant γ_0 is the intrinsic pair creation strength which has been determined from strong decays of baryons as $\gamma_0 = 2.60$ [44].

The strong coupling vertex

$$\langle BC\vec{k}\, lJ \mid T^\dagger \mid A\rangle \; , \tag{4.4}$$

was derived in explicit form in the harmonic oscillator basis [61]. In the present calculations, we use harmonic oscillator wave functions in which there is a single oscillator parameter for the baryons and another one for the mesons which, following [56], are taken to be $\beta_{\rm baryon} = 0.32$ GeV [19] and $\beta_{\rm meson} = 0.40$ (GeV) [52], respectively.

In general, matrix elements of an observable $\hat{\mathcal{O}}$ can be expressed as

$$\mathcal{O} \;=\; \langle \psi_A \mid \hat{\mathcal{O}} \mid \psi_A \rangle \;=\; \mathcal{O}_{\rm val} + \mathcal{O}_{\rm sea} \; , \tag{4.5}$$

where the first term denotes the contribution from the valence quarks

$$\mathcal{O}_{\rm val} \;=\; \mathcal{N}^2 \langle A \mid \hat{\mathcal{O}} \mid A \rangle \; , \tag{4.6}$$

and the second term that from the $q\bar{q}$ pairs

$$\mathcal{O}_{\rm sea} \;=\; \mathcal{N}^2 \sum_{BClJ,B'C'l'J'} \int d\vec{k}\, d\vec{k}\,' \, \frac{\langle A \mid T \mid B'C'\vec{k}\,' l'J' \rangle}{M_A - E_{B'} - E_{C'}} \\ \langle B'C'\vec{k}\,' l'J' \mid \hat{\mathcal{O}} \mid BC\vec{k}\, lJ \rangle \, \frac{\langle BC\vec{k}\, lJ \mid T^\dagger \mid A \rangle}{M_A - E_B - E_C} \; . \tag{4.7}$$

In order to calculate the effects of quark-antiquark pairs on an observable, one has to evaluate the contribution of all possible intermediate states. By using a combination of group theoretical and computational techniques, the sum over intermediate states is carried out up to saturation and not only for the first few shells as in previous studies [51, 56]. Not only does this have a significant impact on the numerical result, but it is necessary for consistency with the OZI-rule and the success of CQMs in hadron spectroscopy. In addition, the contributions of quark-antiquark pairs can be evaluated for any initial baryon (ground state or resonance) and for any flavor of the $q\bar{q}$ pair (not only $s\bar{s}$ as in [56], but also $u\bar{u}$ and $d\bar{d}$), and for any model of baryons and mesons, as long as their wave functions are expressed in the basis of harmonic oscillator wave functions [57, 58].

In this contribution, we use harmonic oscillator wave functions up to five oscillator shells for the intermediate baryons and mesons. All parameters were taken from the literature without attempting to optimize their values in order to improve the agreement with experimental data [57, 58].

4.2 Closure limit

Before discussing an application of the unquenched model to baryon magnetic moments and spins, we study the so-called closure limit in which the intermediate states appearing in Eq. (3.15) are degenerate in energy and hence the energy denominator becomes a constant independent of the quantum numbers of the intermediate states. In the closure limit, the evaluation of the contribution of the quark-antiquark pairs (or the higher Fock components) simplifies considerably, since the sum over intermediate states can be solved by closure and the contribution of the quark-antiquark pairs to the matrix element reduces to

$$\mathcal{O}_{\rm sea} \;\propto\; \langle A \mid T\, \hat{\mathcal{O}}\, T^\dagger \mid A \rangle \; . \tag{4.8}$$

Since the $^3P_0$ pair-creation operator of Eq. (4.2) is a flavor singlet and the energy denominator in Eq. (3.15) is reduced to a constant in the closure limit, the higher Fock component of the baryon wave function has the same flavor symmetry as the valence quark configuration $\mid A\rangle$. Moreover, if the pair-creation operator does not couple to the motion of the valence quarks, the valence quarks act as spectators. In this case, the contribution of the $q\bar{q}$ pairs simplifies further to the expectation value of $\hat{\mathcal{O}}$ between the $^3P_0$ pair states created by $T^\dagger$

$$\mathcal{O}_{\rm sea} \;\propto\; \langle 0 \mid T\, \hat{\mathcal{O}}\, T^\dagger \mid 0 \rangle \; , \tag{4.9}$$

Table 11: Δu, Δd and Δs for ground state octet baryons in the closure limit in units of $(\Delta u)_p/4$.

qqq	$^2 8[56, 0^+]$	Δu	Δd	Δs
uud	p	4	-1	0
udd	n	-1	4	0
uus	Σ^+	4	0	-1
uds	Σ^0	2	2	-1
	Λ	0	0	3
dds	Σ^-	0	4	-1
uss	Ξ^0	-1	0	4
dss	Ξ^-	0	-1	4

the so-called closure-spectator limit [56] which is a special case of the closure limit.

As an example, we discuss the contribution of the quark-antiquark pairs for the operator $2[s_z(q) + s_z(\bar{q})]$ in the closure limit

$$\Delta q \;=\; 2\,\langle s_z(q) + s_z(\bar{q})\rangle \;\; . \tag{4.10}$$

Δq is the nonrelativistic limit of the axial charges and denotes the fraction of the baryon's spin carried by quarks and antiquarks with flavor $q = u,\, d,\, s$. In Table 11 we present the results for the ground state octet baryons with $^2 8[56, 0^+]_{1/2}$. Since the valence-quark configuration of the proton and the neutron does not contain strange quarks, the valence quarks act as spectators in the calculation of Δs. Therefore, the contribution of Δs to the spin of the nucleon is given by the closure-spectator limit which vanishes due to the symmetry properties of the operator Δs and the $^3P_0$ wave function. The same holds for the contribution of $d\bar{d}$ pairs to the Σ^+ and Ξ^0 hyperons, and that of $u\bar{u}$ pairs to the Σ^- and Ξ^- hyperons. The vanishing contributions of Δu and Δd to the spin of the Λ hyperon are a consequence of the Λ wave function in which the up and down quarks are coupled to isospin and spin zero. Similarly, the vanishing contributions of Δq to the spin of the ground state decuplet baryons with $^4 10[56, 0^+]_{3/2}$ in Table 12 can be understood in the closure-spectator limit.

In addition, since in the closure limit the baryon wave function has the same flavor symmetry as the valence quark configuration, it can be shown that the flavor dependence of the contribution of the quark-antiquark pairs to the spin of the ground state baryons in Tables 11 and 12 is the same as that of the valence quarks

$$\Delta u_{\rm sea} : \Delta d_{\rm sea} : \Delta s_{\rm sea} \;=\; \Delta u_{\rm val} : \Delta d_{\rm val} : \Delta s_{\rm val} \;. \tag{4.11}$$

The results for octet and decuplet ground state baryons are related by

$$(\Delta u + \Delta d + \Delta s)_{\rm dec} \;=\; 3\,(\Delta u + \Delta d + \Delta s)_{\rm oct} \;\; . \tag{4.12}$$

Table 12: As Table 11, but for ground state decuplet baryons.

qqq	${}^4 10[56, 0^+]$	Δu	Δd	Δs
uuu	Δ^{++}	9	0	0
uud	Δ^{+}	6	3	0
udd	Δ^{0}	3	6	0
ddd	Δ^{-}	0	9	0
uus	Σ^{*+}	6	0	3
uds	Σ^{*0}	3	3	3
dds	Σ^{*-}	0	6	3
uss	Ξ^{*0}	3	0	6
dss	Ξ^{*-}	0	3	6
sss	Ω^{-}	0	0	9

The same relation holds for the orbital angular momentum

$$(\Delta L)_{\rm dec} \;=\; 3\,(\Delta L)_{\rm oct} \;\;, \tag{4.13}$$

with

$$\Delta L \;=\; \sum_q \Delta L(q) \;=\; \sum_q \langle l_z(q) + l_z(\bar{q})\rangle \;\;. \tag{4.14}$$

Note that, even if the valence quark configuration $[56, 0^+]$ does not carry orbital angular momentum, there is a nonzero contribution of the quark-antiquark pairs in the closure limit, albeit small (less than 1 %) in comparison with that of the quark spins. Obviously, the sum of the spin and orbital parts gives the total angular momentum of the baryon

$$J \;=\; \frac{1}{2}\Delta\Sigma + \Delta L \;\;, \tag{4.15}$$

with

$$\Delta\Sigma \;=\; \Delta u + \Delta d + \Delta s \;\;. \tag{4.16}$$

At a qualitative level, the closure limit helps to explain the phenomenological success of the CQM because the $SU(3)$ flavor symmetry of the baryon wave function is preserved. As an example, the strange content of the proton vanishes in the closure-spectator limit due to many cancelling contributions in the sum over intermediate states in Eq. (3.15). Away from the closure limit, the strangeness content of the proton is expected to be small, in agreement with the experimental data from parity-violating electron scattering (for some recent data see [11, 12]). Even though in this case the cancellations are no longer exact, many intermediate states contribute with opposite signs, and the net result is nonzero, but small. This means that even if the flavor symmetry of the CQM is broken

by the higher Fock components, the net results are still to a large extent determined by the flavor symmetry of the valence quark configuration. Similar arguments were applied to the preservation of the OZI hierarchy in the context of the flux-tube breaking model [54]. Therefore, the closure limit not only provides simple expressions for the relative flavor content of physical observables, but also gives further insight into the origin of cancellations between the contributions from different intermediate states.

In addition, the results in closure limit in Tables 11 and 12 impose very stringent conditions on the numerical calculations, since each entry involves the sum over all possible intermediate states. Therefore, the closure limit provides a highly nontrivial test of the computer codes which involves both the spin-flavor sector, the permutation symmetry, the construction of a complete set of intermediate states in spin-flavor space for each radial excitation and the implementation of the sum over all of these states.

In this section, we discussed some qualitative properties of the unquenched quark model in the closure limit. In the following sections, we study the effects of quark-antiquark pairs on the magnetic moments and the spin of octet baryons in the general case, *i.e.* beyond the closure limit.

4.3 Magnetic moments

The unquenching of the quark model has to be carried out in such a way as to preserve the phenomenological successes of the constituent quark model. In applications to mesons, it was shown that the inclusion of quark-antiquark pairs does not destroy the good CQM results [53] and preserves the OZI hierarchy [54]. In a similar fashion, in this Section I will show that the CQM results for the magnetic moments of the octet baryons also hold in the unquenched constituent quark model (UCQM) [57].

It is well known that the CQM gives a good description of the baryon magnetic moments, even in its simplest form in which the baryons are treated in terms of three constituent quarks in a relative S-wave. The quark magnetic moments are determined by fitting the magnetic moments of the proton, neutron and Λ hyperon to give $\mu_u = 1.852$, $\mu_d = -0.972$ and $\mu_s = -0.613\ \mu_N$ [2].

In the unquenched CQM the baryon magnetic moments also receive contributions from the quark spins of the pairs and the orbital motion of the quarks

$$\vec{\mu} \ = \ \sum_q \mu_q \left[2\vec{s}(q) + \vec{l}(q) - 2\vec{s}(\bar{q}) - \vec{l}(\bar{q}) \right] \ , \tag{4.17}$$

where $\mu_q = e_q \hbar / 2 m_q c$ is the quark magnetic moment. In Fig. 14 we show a comparison between the experimental values of the magnetic moments of the octet baryons (circles) and the theoretical values obtained in the CQM (squares) and in the unquenched quark model (triangles). The results for the unquenched quark model were obtained in a calculation involving a sum over intermediate states up to five oscillator shells for both baryons and mesons. We note, that the results for the magnetic moments, after renormalization, are almost independent on the number of shells included in the sum over intermediate states. The values of the magnetic moments in the unquenched quark model are very similar to

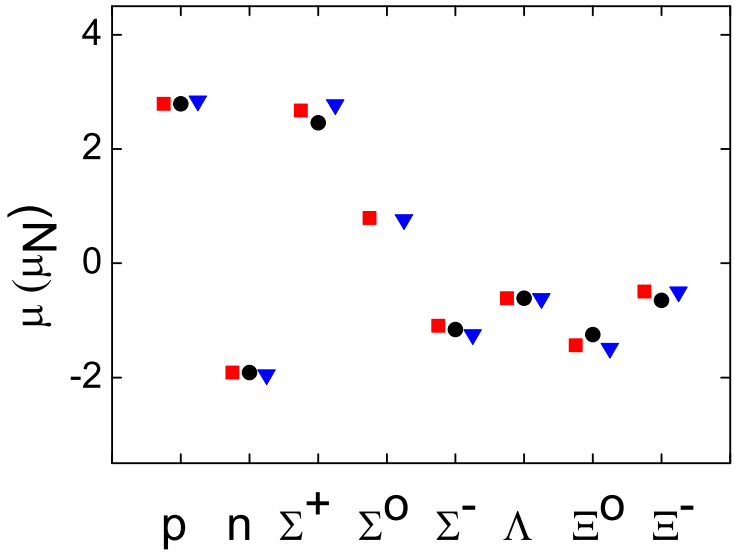

Figure 14: Magnetic moments of octet baryons: experimental values from PDG [2] (circles), CQM (squares) and unquenched quark model (triangles).

those in the CQM. The largest difference is observed for the charged Σ hyperons, but the relation between the magnetic moments of Σ hyperons [63], $\mu(\Sigma^0) = [\mu(\Sigma^+) + \mu(\Sigma^-)]/2$, is preserved in the unquenched calculation due to isospin symmetry.

The inclusion of the $q\bar{q}$ pairs leads to slightly different values of the quark magnetic moments, $\mu_u = 2.066$, $\mu_d = -1.110$ and $\mu_s = -0.633$ μ_N as for the CQM. This is related to the well-known phenomenon, that a calculation carried out in a truncated basis leads to effective parameters in order to reproduce the results obtained in a more extended basis. The results in the unquenched quark model are practically identical, after renormalization, to the ones in the CQM, which shows that the addition of the quark-antiquark pairs preserves the good CQM results for the baryon magnetic moments. A similar feature was found in the context of the flux-tube breaking model for mesons in which it was shown that the inclusion of quark-antiquark pairs preserved the linear behavior of the confining potential as well as the OZI hierarchy [54]. The change in the linear potential caused by the bubbling of the pairs in the string could be absorbed into a renormalized strength of the linear potential.

The results for the magnetic moments can be understood qualitatively in the closure limit in which the relative contribution of the quark spins from the quark-antiquark pairs is the same as that from the valence quarks. Moreover, since in the closure limit the contribution of the orbital angular momentum is small in comparison to that of the quark spins, the results for the baryon magnetic moments are almost indistinguishable from those of the CQM. Away from the closure limit, even though the relations between the different contributions no longer hold exactly, they are still valid approximately. In

addition, there is now a contribution from the orbital part (at the level of ~ 5 %) which is mainly due to the baryon-pion channel.

In summary, the inclusion of the effects of quark-antiquark pairs preserves, after renormalization, the good results of the CQM for the magnetic moments of the octet baryons.

4.4 Flavor content

The flavor asymmetry of the proton $\mathcal{A}(p)$ is related to the Gottfried integral S_G for the difference of the proton and neutron electromagnetic structure functions as

$$S_G \;=\; \int_0^1 \frac{F_2^p(x) - F_2^n(x)}{x} dx \;=\; \frac{1}{3} - \frac{2}{3}\int_0^1 \left[\bar{d}_p(x) - \bar{u}_p(x)\right] dx \;=\; \frac{1}{3}[1 - 2\mathcal{A}(p)] \;. \quad (4.18)$$

Under the assumption of a flavor symmetric (or rather flavor independent) sea one obtains the Gottfried sum rule $S_G = 1/3$ [10, 64], whereas any deviation from this value is an indication of the $\bar{d}/\bar{u}$ asymmetry of the nucleon sea, thus providing evidence of the existence of higher Fock components (such as $qqq - q\bar{q}$ configurations) in the proton wave function. The first clear evidence of a violation of the Gottfried sum rule came from the New Muon Collaboration (NMC) [65] which was later confirmed by Drell-Yan experiments [66, 67] and a measurement of semi-inclusive deep-inelastic scattering [68]. All experiments show evidence that there are more $\bar{d}$ quarks in the proton than there are $\bar{u}$ quarks [10]. The final NMC value is 0.2281 ± 0.0065 at $Q^2 = 4$ (GeV/c)^2 for the Gottfried integral over the range $0.004 \leq x \leq 0.8$ [65], which implies a flavor asymmetric sea. The observed flavor asymmetry is far too large to be accounted for by processes that can be described by QCD in perturbative regime and therefore has to attributed to non-perturbative QCD mechanisms. It was shown in the framework of the meson-cloud model, that the coupling of the nucleon to the pion cloud provides a mechanism that is able to produce a flavor asymmetry due to the dominance of $n\pi^+$ among the virtual configurations [69].

In the unquenched quark model, the flavor asymmetry of the proton can be calculated directly from the difference of the number of $\bar{d}$ and $\bar{u}$ sea quarks in the proton, even in the absence of explicit information on the (anti)quark distribution functions. Table 13 shows that the flavor asymmetry for the proton in the UCQM is 0.151 which corresponds to a value of the Gottfried integral of 0.232, remarkably close to the experimental value. The main contribution to the flavor asymmetry of the proton is due to the pion loops, especially the $n\pi^+$ intermediate state, thus confirming in an explicit calculation the explanation given in Ref. [69] in the context of the meson-cloud model. In addition, we find that there are important contributions from the $\Delta\pi$ channel and, especially, from the off-diagonal terms $p\pi^0$-$p\eta_8$ and $p\pi^0$-$p\eta_1$ which together are of the order of 15-20 % of that of the $N\pi$ channel, but with the opposite sign (see Table 13). The contribution of the intermediate vector mesons is very small due to a cancelation between the $n\rho^+$ and the $\Delta\rho$ channels and the cross terms $p\rho^0$-$p\omega_8$ and $p\rho^0$-$p\omega_1$. Kaon loops do not contribute to the proton flavor asymmetry. Table 13 shows that the full four-shell calculation is dominated by the contribution of the ground state intermediate baryons and mesons (0 $\hbar\omega$). Both

Table 13: Contributions to the flavor asymmetry of the proton [58]. $N^2 = 1 + a^2 + b^2 + c^2 + d^2$ is the normalization factor of the wave function of Eq. (4.19).

	Unquenched QM		Meson-Cloud
	0-4 $\hbar\omega$	0 $\hbar\omega$	Eq. (4.20)
$N\pi$	0.195	0.177	$2a^2/3N^2$
$\Delta\pi$	–0.016	–0.010	$-b^2/3N^2$
$N\pi\eta_8\eta_1$	–0.028	–0.018	$-2a(c+d\sqrt{2})/3N^2$
$N\rho$	0.050	0.012	
$\Delta\rho$	–0.017	–0.003	
$N\rho\omega_8\omega_1$	–0.033	–0.010	
Total	0.151	0.147	

columns show the same qualitative behavior: dominance of the pion loops with a small negative correction of the order of 10-15 % due to the off-diagonal terms involving π and η pseudoscalar mesons and an almost vanishing contribution from the vector mesons.

A similar result can be obtained in the meson-cloud model by considering a proton wave function including not only pion loops but also eta loops

$$\begin{aligned} |\psi_p\rangle \;\; \rightarrow \;\; |p\rangle + a\left[\frac{1}{\sqrt{3}}\,|p\pi^0\rangle - \sqrt{\frac{2}{3}}\,|n\pi^+\rangle\right] + c\,|N\eta_8\rangle + d\,|N\eta_1\rangle \\ + b\left[\frac{1}{\sqrt{2}}\,|\Delta^{++}\pi^-\rangle - \frac{1}{\sqrt{3}}\,|\Delta^+\pi^0\rangle + \frac{1}{\sqrt{6}}\,|\Delta^0\pi^+\rangle\right] . \end{aligned} \tag{4.19}$$

In the last column of Table 13 we show the contributions of the different terms of Eq. (4.19) to the flavor asymmetry of the proton to obtain

$$\mathcal{A}(p) \;=\; \frac{2a^2 - b^2 - 2a(c + d\sqrt{2})}{3(1 + a^2 + b^2 + c^2 + d^2)} \; . \tag{4.20}$$

Since the unquenched quark model is valid not only for the proton, but for all baryons (ground state or resonance), it is straightforward to calculate the flavor asymmetries of the other octet baryons. For the Σ^+ hyperon and the Ξ^0 cascade particle we find $\mathcal{A}(\Sigma^+) = 0.126$ and $\mathcal{A}(\Xi^0) = -0.001$ [58], respectively. The flavor asymmetries of the remaining octet baryons can be obtained by using the isospin symmetry of the unquenched quark model [58]. For example, the excess of $\bar{d}$ over $\bar{u}$ in the proton is related to the excess of $\bar{u}$ over $\bar{d}$ in the neutron, $\mathcal{A}(p) = -\mathcal{A}(n)$. Similar relations hold for the other octet baryons: $\mathcal{A}(\Sigma^+) = -\mathcal{A}(\Sigma^-)$, $\mathcal{A}(\Xi^0) = -\mathcal{A}(\Xi^-)$ and $\mathcal{A}(\Lambda) = \mathcal{A}(\Sigma^0) = 0$. Just as for the proton, the flavor asymmetry of the other octet baryons is expected to be dominated by pion loops, whereas the other contributions are suppressed by the energy denominator in Eq. (4.1). For the Σ hyperon this is indeed the case, but for the cascade particles the pion loops are suppressed by the value of the $SU(3)$ flavor coupling which is a factor

Table 14: Relative flavor asymmetries of octet baryons

Model	$\mathcal{A}(\Sigma^+)/\mathcal{A}(p)$	$\mathcal{A}(\Xi^0)/\mathcal{A}(p)$	Ref.
Unquenched CQM	0.833	–0.005	[58]
Octet couplings	0.353	–0.647	[72]
Chiral QM	2	1	[70]
Balance Model	3.083	2.075	[71]

of 5 smaller than that for the proton. Hence for the Ξ hyperons there is no dominant contribution. Since for the Ξ hyperon all contributions are roughly of the same order and small, and moreover some with a positive and others with a negative sign, the value of the flavor asymmetry of the cascade particles is calculated to be small [58].

In Table 14, we show a comparison of some predictions for the flavor asymmetry of the Σ^+ and Ξ^0 hyperons relative to that of the proton. In the unquenched quark model, the flavor asymmetry of the proton is predicted to be of the same order as that of the Σ^+ hyperon and much larger than that of the cascade particle

$$\mathcal{A}(p) \sim \mathcal{A}(\Sigma^+) \gg |\mathcal{A}(\Xi^0)| . \tag{4.21}$$

This behavior is very different from that obtained in the chiral quark model $\mathcal{A}(\Sigma^+) = 2\mathcal{A}(p) = 2\mathcal{A}(\Xi^0)$ [70], the balance model $\mathcal{A}(\Sigma^+) > \mathcal{A}(\Xi^0) > \mathcal{A}(p)$ [71], and the octet model $\mathcal{A}(p) > |\mathcal{A}(\Xi^0)| > \mathcal{A}(\Sigma^+)$ [72]. The values for the chiral quark model and the balance model were taken from [73].

In order to distinguish between the predictions of the different models and to obtain a better understanding of the non-perturbative structure of QCD, new experiments are needed to measure the flavor asymmetry of hyperons. In particular, the flavor asymmetry of charged Σ hyperons can obtained from Drell-Yan experiments using charged hyperon beams on the proton [72] or by means of backward $K^\pm$ electroproduction [74].

4.5 Spin content

The contribution of the quark spins to the spin of the proton can be obtained from the proton spin structure function g_1^p in combination with the neutron and hyperon semileptonic decays [46]. The observation by the European Muon Collaboration that the total quark spin constitutes only a small fraction of the spin of the nucleon [45] sparked an enormous interest in the spin structure of the proton [46]. Recent experiments show that approximately one third of the proton spin is carried by quarks [75, 76], and that the gluon contribution is rather small (either positive or negative) and compatible with zero [77]. This rules out the possibility that most of the missing spin be carried by the gluon and indicates that the origen of the missing spin of the proton has to be attributed to other mechanisms.

In the unquenched quark model, the effect of hadron loops on the fraction of the proton spin carried by the quark (antiquark) spins and orbital angular momentum can be

Table 15: Contribution of quark spins $\Delta\Sigma$ and orbital angular momentum ΔL to the spin of the proton and the Λ hyperon

		CQM	Unquenched QM		
			Valence	Sea	Total
p	$\Delta\Sigma$	1	0.378	0.298	0.676
	$2\Delta L$	0	0.000	0.324	0.324
	$2\Delta J$	1	0.378	0.622	1.000
Λ	$\Delta\Sigma$	1	0.422	0.429	0.851
	$2\Delta L$	0	0.000	0.149	0.149
	$2\Delta J$	1	0.422	0.578	1.000

studied in an explicit way [57]. As in other effective models [46], gluonic effects associated with the axial anomaly are not included, and therefore the contribution from the gluons is missing from the outset. The total spin of the proton can then be written as the sum of the contributions from the quark (and antiquark) spins and orbital angular momentum

$$1 \;=\; 2\Delta J \;=\; \Delta\Sigma + 2\Delta L \;. \tag{4.22}$$

Table 15 shows that the inclusion of the quark-antiquark pairs has a dramatic effect on the spin content of the proton. Whereas in the CQM the proton spin is carried entirely by the (valence) quarks, in the unquenched calculation the contributions of the valence quark spins, the sea quark spins and the orbital angular momentum to the proton spin are comparable in size and equal to approximately 38, 30 and 32 %, respectively. The importance of orbital angular momentum to the proton spin was discussed many years ago by Sehgal [78] and Ratcliffe [79] in the context of the quark-parton model and, more recently, by Myhrer and Thomas in framework of the bag model [80].

These results can be understood in a qualitative way by considering the proton wave function of Eq. (4.19), whose contribution to the orbital angular momentum can be derived as

$$\Delta L \;=\; \frac{2a^2 - b^2 + 2c^2 + 2d^2}{3(1 + a^2 + b^2 + c^2 + d^2)} \;. \tag{4.23}$$

The effects of pion loops for the proton flavor asymmetry and the contribution of orbital angular momentum to the proton spin are identical $\mathcal{A}(p) = \Delta L$ as a consequence of the spin and isospin properties [81]. Since in the unquenched calculations both the flavor asymmetry and the orbital angular momentum are dominated by pion loops (see Tables 13 and 16), this relation is to a good approximation still valid in the UCQM, $\mathcal{A}(p) = 0.151$ and $\Delta L = 0.162$, respectively. Table 16 shows that, just as for the flavor asymmetry, the orbital angular momentum is dominated by the contribution of the ground state intermediate baryons and mesons (0 $\hbar\omega$) and in particular by the $N\pi$ channel. The

Table 16: Contribution of the orbital angular momentum $2\Delta L$ to the spin of the proton. $N^2 = 1 + a^2 + b^2 + c^2 + d^2$ is the normalization factor of the wave function of Eq. (4.19).

	Unquenched QM		Meson-Cloud
	0-5 $\hbar\omega$	0 $\hbar\omega$	Eq. (4.23)
$N\pi$	0.370	0.336	$4a^2/3N^2$
$\Delta\pi$	–0.027	–0.020	$-2b^2/3N^2$
$N\eta_8$, $N\eta_1$	0.007	0.0012	$4(c^2+d^2)/3N^2$
ΣK, ΛK	0.016	0.004	
Pseudoscalar	0.367	0.321	
Vector	–0.043	–0.011	
Total	0.324	0.310	

contributions of the eta and kaon loops to the orbital angular momentum, as well as that of the vector mesons, are small with respect to that of the pions.

The situation for the quark spins is completely different. In the unquenched calculations, the contributions of valence and sea quarks are given by $\Delta\Sigma_{\rm val} = 0.378$ and $\Delta\Sigma_{\rm sea} = 0.298$, respectively. While the orbital angular momentum arises almost entirely from the $N\pi$ channel, the sea quark spins are dominated by the intermediate vector mesons with a very small contribution from the pseudoscalar mesons (see second column of Table 17). The third column of Table 17 shows that the contribution of the ground state intermediate baryons and mesons (0 $\hbar\omega$) is small for both the pseudoscalar and vector mesons, whereas the full calculation is dominated by the contribution of the vector mesons. This shows that for the sea quark spins it is crucial to include the effects of the excited vector mesons which makes the convergence of the sum over intermediate states is much slower. Therefore, the sum was carried out over five complete oscillator shells for both the intermediate baryons and mesons [57].

In a simple meson-cloud model based on ground state baryons and mesons only, the contribution of the sea quark spins is very small. For example, for the proton wave function of Eq. (4.19) in which only pion and eta loops are taken into account, the contribution of the quark spins is given by $\Delta\Sigma = \Delta\Sigma_{\rm val} + \Delta\Sigma_{\rm sea} = 1 - 2\Delta L$ with

$$\begin{aligned} \Delta\Sigma_{\rm val} &= \frac{1}{1 + a^2 + b^2 + c^2 + d^2} \,, \\ \Delta\Sigma_{\rm sea} &= \frac{-a^2 + 5b^2 - c^2 - d^2}{3(1 + a^2 + b^2 + c^2 + d^2)} \,. \end{aligned} \tag{4.24}$$

With the values of the coefficients a, b, c and d, as determined by comparing the third and fourth columns of Tables 16 and 17, we find that for this case the contribution of the sea quark spins is very small $\Delta\Sigma_{\rm sea} = -0.035$.

The experimental data on the spin structure of the proton have raised many questions about the contributions of valence and sea quarks, gluons and orbital angular momentum

Table 17: Contribution of the sea quark spins $\Delta\Sigma_{\rm sea}$ to the spin of the proton

	Unquenched QM		Meson-Cloud
	0-5 $\hbar\omega$	0 $\hbar\omega$	Eq. (4.24)
$N\pi$	–0.089	–0.084	$-a^2/3N^2$
$\Delta\pi$	0.074	0.049	$5b^2/3N^2$
$N\eta_8$, $N\eta_1$	0.006	–0.0003	$-(c^2+d^2)/3N^2$
ΣK, ΛK	0.013	0.002	
Pseudoscalar	0.005	–0.033	
Vector	0.293	0.052	
Total	0.298	0.019	

to the proton spin. In this respect it is of interest to investigate the spin structure of other octet baryons, in particular the Λ hyperon. In most studies, additional assumptions had to be made about the sea quarks in order to get an estimate of its spin content. For example, the assumption that both valence and sea quarks are related by $SU(3)$ flavor symmetry, allows to express the spin content of the Λ hyperon in terms of that of the proton [82, 83, 84] and gives rise to equal contributions of the quark spins $(\Delta\Sigma)_\Lambda = (\Delta\Sigma)_p$. In the unquenched quark model there is no need to make additional assumptions about the nature of the sea. Table 15 shows that the contribution of quark spins for the Λ is larger than that for the proton, $(\Delta\Sigma)_\Lambda > (\Delta\Sigma)_p$, which is a result of $SU(3)$ flavor breaking by the sea quarks.

5 Summary and conclusions

In these lecture notes, I discussed some general features of quark models based on three valence quarks, in particular, a stringlike collective model in which the baryons (three-quark configurations) are interpreted as rotations and vibrations of the strings. In spite of the successes of quark models in general in describing masses, magnetic moments, electromagnetic and strong couplings, there are some systematic discrepancies with the experimental data on electromagnetic and strong couplings that cannot be explained in any quark model based on valence quarks only. These observations, in combination with more direct experimental evidence for the importance of exotic (*i.e.* non qqq) degrees of freedom in baryons, has led to the development of an extension of the quark model, the so-called unquenched quark model,

In the second part, I presented an unquenched quark model for baryons in which the effects of sea quarks are taken into account in an explicit form via a microscopic, QCD-inspired, creation mechanism of the quark-antiquark pairs ($u\bar{u}$, $d\bar{d}$ and $s\bar{s}$). As an application, I studied the spin and flavor content of the proton and presented an analysis of the numerical results by means of a simple exactly solvable meson-cloud model including

pion and eta loops.

The inclusion of the $q\bar{q}$ pairs leads automatically to an excess of $\bar{d}$ over $\bar{u}$ quarks, in agreement with the observed flavor asymmetry of the proton. The results for the flavor asymmetry of the proton are dominated by the $N\pi$ channel, but with important contributions from the $\Delta\pi$ channel and the off-diagonal $N\pi$-$N\eta$ terms. The contributions from orbitally excited intermediate baryons and mesons is small.

Similarly, the inclusion of hadron loops leads to a sizeable contribution of the orbital angular momentum to the spin of the proton (~ 32 %). Just as in the case of the flavor asymmetry, the contribution of orbital angular momentum to the spin of the proton is dominated by pion loops with relatively small contributions from the other channels. However, the contribution of sea quark spins to the spin of the proton (~ 30 %) is almost entirely due to excited vector mesons. We note, that the latter contribution is absent in meson-cloud models.

Even though different models of hadron structure may show similar results for the properties of the proton, often their predictions for the other octet baryons exhibit large variations. Therefore, in order to be able to distinguish between the predictions of different models of hadron structure and to obtain a better understanding of the non-perturbative structure of QCD new experiments are needed to measure the flavor asymmetry and spin content of other octet baryons.

The results for the magnetic moments and the spin and flavor content of octet baryons are very promising and encouraging. The inclusion of the effects of quark-antiquark pairs in a general and consistent way, as suggested here, may provide a major improvement to the constituent quark model which increases considerably its range of applicability.

Acknowledgments

These lecture notes are based in part on the lecture notes on *The structure of the nucleon: baryons and pentaquarks* published in the proceedings of the *IV Escuela Mexicana de Física Nuclear* [85] and in part on several articles [57, 58] and a conference proceedings [59, 60].

The results presented in these lectures notes were obtained in collaboration with Franco Iachello, Ami Leviatan, Elena Santopinto, Jacopo Ferretti, Hugo García Tecocoatzi and Miguel Ángel López Ruiz. This work is supported in part by grants from CONACyT (78833) and PAPIIT-DGAPA (IN113711), Mexico.

A Baryon spin-flavor wave functions

Here we list the conventions used for the spin and flavor wave functions which are consistent with the choice of Jacobi coordinates of Eq. (3.1). They coincide with the conventions of [22, 86].

A.1 Spin wave functions

The spin of q^3 baryons can be either $S = \frac{3}{2}$ or $S = \frac{1}{2}$ with A_1 or E symmetry under D_3, respectively. The corresponding spin wave functions $|S, M_S\rangle$ are given by [22, 86]

$$\begin{array}{rcccl} \left|\frac{3}{2},\frac{3}{2}\right\rangle & : & \chi_{A_1} & = & |\uparrow\uparrow\uparrow\rangle \\ \left|\frac{1}{2},\frac{1}{2}\right\rangle & : & \chi_{E_\rho} & = & \frac{1}{\sqrt{2}}\left[|\uparrow\downarrow\uparrow\rangle - |\downarrow\uparrow\uparrow\rangle\right] \\ & : & \chi_{E_\lambda} & = & \frac{1}{\sqrt{6}}\left[2\,|\uparrow\uparrow\downarrow\rangle - |\uparrow\downarrow\uparrow\rangle - |\downarrow\uparrow\uparrow\rangle\right] \end{array} \tag{A.1}$$

We only show the state with the largest component of the projection $M_S = S$. The other states with $-S \leq M_S < S$ are obtained by applying the lowering operator in spin space.

A.2 Flavor wave functions

The states of a $SU(3)$ flavor multiplet characterized by $(p, q) = (f_1 - f_2, f_2 - f_3)$ are labeled by the isospin I, its projection I_3 and the hypercharge Y. The flavor multiplets of q^3 baryons are characterized by $(p, q) = (1, 1)$ (octet), $(3, 0)$ (decuplet) and $(0, 0)$ (singlet) with A_1, E and A_2 symmetry under D_3, respectively. The corresponding flavor wave functions $|(p, q), I, I_3, Y\rangle$ are obtained using the phase convention of De Swart [87] and agree with the ones given in Refs. [22, 86]. The flavor wave functions of baryons are given by

$$\begin{array}{rcccl} \left|(3,0),\frac{3}{2},\frac{3}{2},1\right\rangle & : & \phi_{A_1}(\Delta^{++}) & = & |uuu\rangle \\ |(3,0),1,1,0\rangle & : & \phi_{A_1}(\Sigma^{+}) & = & \frac{1}{\sqrt{3}}[|suu\rangle + |usu\rangle + |uus\rangle] \\ \left|(3,0),\frac{1}{2},\frac{1}{2},-1\right\rangle & : & \phi_{A_1}(\Xi^{0}) & = & \frac{1}{\sqrt{3}}[|ssu\rangle + |sus\rangle + |uss\rangle] \\ |(3,0),0,0,-2\rangle & : & \phi_{A_1}(\Omega^{-}) & = & |sss\rangle \end{array} \tag{A.2}$$

for decuplet baryons with $(p,q)=(3,0)$,

$$\begin{array}{lcll}
\left|(1,1),\frac{1}{2},\frac{1}{2},1\right\rangle & : & \phi_{E_\rho}(p) & = \frac{1}{\sqrt{2}}[|udu\rangle - |duu\rangle] \\
 & : & \phi_{E_\lambda}(p) & = \frac{1}{\sqrt{6}}[2|uud\rangle - |udu\rangle - |duu\rangle] \\
|(1,1),1,1,0\rangle & : & \phi_{E_\rho}(\Sigma^+) & = \frac{1}{\sqrt{2}}[|suu\rangle - |usu\rangle] \\
 & : & \phi_{E_\lambda}(\Sigma^+) & = \frac{1}{\sqrt{6}}[|suu\rangle + |usu\rangle - 2|uus\rangle] \\
|(1,1),0,0,0\rangle & : & \phi_{E_\rho}(\Lambda) & = \frac{1}{\sqrt{12}}[2|uds\rangle - 2|dus\rangle - |dsu\rangle \\
 & & & \qquad +|sdu\rangle - |sud\rangle + |usd\rangle] \\
 & : & \phi_{E_\lambda}(\Lambda) & = \frac{1}{2}[-|dsu\rangle - |sdu\rangle + |sud\rangle + |usd\rangle] \\
\left|(1,1),\frac{1}{2},\frac{1}{2},-1\right\rangle & : & \phi_{E_\rho}(\Xi^0) & = \frac{1}{\sqrt{2}}[|sus\rangle - |uss\rangle] \\
 & : & \phi_{E_\lambda}(\Xi^0) & = \frac{1}{\sqrt{6}}[2|ssu\rangle - |sus\rangle - |uss\rangle]
\end{array} \tag{A.3}$$

for octet baryons with $(p,q)=(1,1)$, and

$$|(0,0),0,0,0\rangle \;:\; \phi_{A_2}(\Lambda) \;=\; \frac{1}{\sqrt{6}}[|uds\rangle - |dus\rangle + |dsu\rangle - |sdu\rangle + |sud\rangle - |usd\rangle] \tag{A.4}$$

for singlet baryons with $(p,q)=(0,0)$. In Eqs. (A.2-A.4) we show the highest charge state $I_3 = I$ with $Q = I_3 + \frac{Y}{2}$. The other charge states with $-I \le I_3 < I$ are obtained by applying the lowering operator in isospin space. Note that the flavor wave functions of the Δ^{++} (decuplet) and proton (octet) are related to the spin wave functions of Eq. (A.1) by interchanging u (d) by $\uparrow$ ($\downarrow$).

B Meson spin-flavor wave functions

Here we list the spin and flavor wave functions of mesons. They coincide with the conventions of [87, 88].

B.1 Spin wave functions

The spin of $q\bar{q}$ mesons can be either $S=0$ or $S=1$. The corresponding spin wave functions $|S,M_S\rangle$ are given by

$$\begin{array}{lcll}
|0,0\rangle & : & \chi_0 & = \frac{1}{\sqrt{2}}\left[|\uparrow\downarrow\rangle - |\downarrow\uparrow\rangle\right] \\
|1,1\rangle & : & \chi_1 & = |\uparrow\uparrow\rangle
\end{array} \tag{B.1}$$

We only show the state with the largest component of the projection $M_S = S$. The other states with $-S \le M_S < S$ are obtained by applying the lowering operator in spin space.

B.2 Flavor wave functions

The states of a $SU(3)$ flavor multiplet characterized by $(p,q)=(f_1-f_2, f_2-f_3)$ are labeled by the isospin I, its projection I_3 and the hypercharge Y. The flavor multiplets of $q\bar{q}$

mesons are characterized by $(p,q) = (1,1)$ (octet) and $(0,0)$ (singlet). The corresponding flavor wave functions $|(p,q), I, I_3, Y\rangle$ are obtained using the phase convention of De Swart [87] and agree with the ones given in Ref. [88]. The flavor wave functions of mesons are given by

$$\begin{array}{lcll}
\left|(1,1),\frac{1}{2},\frac{1}{2},1\right\rangle & : & \phi(K^+) & = -|u\bar{s}\rangle \\
\left|(1,1),\frac{1}{2},-\frac{1}{2},1\right\rangle & : & \phi(K^0) & = -|d\bar{s}\rangle \\
|(1,1),1,1,0\rangle & : & \phi(\pi^+) & = -|u\bar{d}\rangle \\
|(1,1),1,0,0\rangle & : & \phi(\pi^0) & = \frac{1}{\sqrt{2}}[|u\bar{u}\rangle - |d\bar{d}\rangle] \\
|(1,1),1,-1,0\rangle & : & \phi(\pi^-) & = |d\bar{u}\rangle \\
|(1,1),0,0,0\rangle & : & \phi(\eta_8) & = \frac{1}{\sqrt{6}}[|u\bar{u}\rangle + |d\bar{d}\rangle - 2|s\bar{s}\rangle] \\
\left|(1,1),\frac{1}{2},\frac{1}{2},-1\right\rangle & : & \phi(\overline{K}^0) & = -|s\bar{d}\rangle \\
\left|(1,1),\frac{1}{2},\frac{1}{2},-1\right\rangle & : & \phi(K^-) & = |s\bar{u}\rangle
\end{array} \tag{B.2}$$

for the octet mesons with $(p,q) = (1,1)$, and

$$|(0,0),0,0,0\rangle \;:\; \phi(\eta_1) \;=\; \tfrac{1}{\sqrt{3}}[|u\bar{u}\rangle + |d\bar{d}\rangle + |s\bar{s}\rangle] \tag{B.3}$$

for the singlet meson with $(p,q) = (0,0)$.

C Baryon wave functions

The S_3 invariant space-spin-flavor ($\Psi = \psi\chi\phi$) baryon wave functions are given by

$$\begin{array}{rcl}
^2 8[56, L^P] & : & \frac{1}{\sqrt{2}}\psi_{A_1}(\chi_{E_\rho}\phi_{E_\rho} + \chi_{E_\lambda}\phi_{E_\lambda}) \\
^2 8[70, L^P] & : & \frac{1}{2}[\psi_{E_\rho}(\chi_{E_\rho}\phi_{E_\lambda} + \chi_{E_\lambda}\phi_{E_\rho}) + \psi_{E_\lambda}(\chi_{E_\rho}\phi_{E_\rho} - \chi_{E_\lambda}\phi_{E_\lambda})] \\
^4 8[70, L^P] & : & \frac{1}{\sqrt{2}}(\psi_{E_\rho}\phi_{E_\rho} + \psi_{E_\lambda}\phi_{E_\lambda})\chi_{A_1} \\
^2 8[20, L^P] & : & \frac{1}{\sqrt{2}}\psi_{A_2}(\chi_{E_\rho}\phi_{E_\lambda} - \chi_{E_\lambda}\phi_{E_\rho}) \\
^4 10[56, L^P] & : & \psi_{A_1}\chi_{A_1}\phi_{A_1} \\
^2 10[70, L^P] & : & \frac{1}{\sqrt{2}}(\psi_{E_\rho}\chi_{E_\rho} + \psi_{E_\lambda}\chi_{E_\lambda})\phi_{A_1} \\
^2 1[70, L^P] & : & \frac{1}{\sqrt{2}}(\psi_{E_\rho}\chi_{E_\lambda} - \psi_{E_\lambda}\chi_{E_\rho})\phi_{A_2} \\
^4 1[20, L^P] & : & \psi_{A_2}\chi_{A_1}\phi_{A_2}
\end{array} \tag{C.1}$$

The quark orbital angular momentum L is coupled with the spin S to the total angular momentum J of the baryon.

References

[1] I. Estermann, R. Frisch and O. Stern, Nature **132**, 169 (1933).

[2] K. Nakamura *et al.*, J. Phys. G: Nucl. Part. Phys. **37**, 075021 (2010).

[3] R. Hofstadter, Annu. Rev. Nucl. Sci. **7**, 231 (1957).

[4] J.I. Friedman and H.W. Kendall, Annu. Rev. Nucl. Sci. **22**, 203 (1972).

[5] M.K. Jones *et al.*, Phys. Rev. Lett. **84**, 1398 (2000);
O. Gayou *et al.*, Phys. Rev. Lett. **88**, 092301 (2002).

[6] See *e.g.* C.E. Hyde-Wright and K. de Jager, Annu. Rev. Nucl. Part. Sci. **54**, 217 (2004).

[7] See *e.g.* V.D. Burkert and T.-S.H. Lee, Int. J. Mod. Phys. E **13**, 1035 (2004) [arXiv:nucl-ex/0407020].

[8] M. Gell-Mann and Y. Ne'eman, *The Eightfold Way*, (W.A. Benjamin, New York, 1964).

[9] S. Kumano, Phys. Rep. **303**, 183 (1998).

[10] G.T. Garvey and J.-C. Peng, Prog. Part. Nucl. Phys. **47**, 203 (2001).

[11] A. Acha *et al* Phys. Rev. Lett. **98**, 032301 (2007).

[12] S. Baunack *et al*, Phys. Rev. Lett. **102**, 151803 (2009).

[13] M. Hamermesh, *Group theory and its application to physical problems*, (Dover Publications, New York, 1989).

[14] F.E. Close, *An introduction to quarks and partons*, (Academic Press, London, 1979)

[15] Fl. Stancu, *Group theory in subnuclear physics*, (Oxford University Press, Oxford, 1996).

[16] N. Isgur, Nucl. Phys. A **623**, 37c (1997).

[17] A.W. Thomas and W. Weise, *The structure of the nucleon* (Wiley-VCH, Berlin, 2001);
S. Theberge and A.W. Thomas, Nucl. Phys. A **393**, 252 (1983);
A.W. Thomas, Phys. Lett. B **126**, 97 (1983).

[18] T. Schaefer and E. Shuryak, Phys. Rev. D **53**, 6522 (1996); Rev. Mod. Phys. **70** 323 (1998);
D. Diakonov, Prog. Part. Nucl. Phys. **51**, 173 (2003).

[19] N. Isgur and G. Karl, Phys. Rev. D **18**, 4187 (1978); *ibid.* **19**, 2653 (1979); *ibid.* **20**, 1191 (1979).

[20] S. Capstick and N. Isgur, Phys. Rev. D **34**, 2809 (1986).

[21] R. Bijker, F. Iachello and A. Leviatan, Ann. Phys. (N.Y.) **236**, 69 (1994).

[22] R. Bijker, F. Iachello and A. Leviatan, Ann. Phys. (N.Y.) **284**, 89 (2000).

[23] M. Ferraris, M.M. Giannini, M. Pizzo, E. Santopinto and L. Tiator, Phys. Lett. B **364**, 231 (1995);
M. Aiello, M. Ferraris, M.M. Giannini, M. Pizzo and E. Santopinto, Phys. Lett. B **387**, 215 (1996);
M. Aiello, M.M. Giannini and E. Santopinto, J. Phys. G: Nucl. Part. Phys. **24**, 753 (1998).

[24] L.Ya. Glozman and D.O. Riska, Phys. Rep. **268**, 263 (1996);
L.Ya. Glozman, Z. Papp, W. Plessas, K. Varga and R.F. Wagenbrunn, Phys. Rev. C **57**, 3406 (1998);
L.Ya. Glozman, W. Plessas, K. Varga and R.F. Wagenbrunn, Phys. Rev. D **58**, 094030 (1998).

[25] U. Löring, K. Kretzschmar, B.Ch. Metsch and H.R. Petry, Eur. Phys. J. A **10**, 309 (2001);
U. Löring, B.Ch. Metsch and H.R. Petry, Eur. Phys. J. A **10**, 395 (2001); *ibid.* **10**, 447 (2001).

[26] S. Capstick and W. Roberts, Prog. Part. Nucl. Phys. **45**, S241 (2000).

[27] F. Iachello, N.C. Mukhopadhyay and L. Zhang, Phys. Lett. B **256**, 295 (1991); Phys. Rev. D **44**, 898 (1991).

[28] K. Johnson and C.B. Thorn, Phys. Rev. D **13**, 1934 (1974);
I. Bars and A.J. Hanson, Phys. Rev.D **13**, 1744 (1974).

[29] F. Gürsey and L.A. Radicati , Phys. Rev. Lett. **13**, 173 (1964).

[30] L.Ya. Glozman, W. Plessas, K. Varga and R.F. Wagenbrunn, *Phys. Rev. D* **58** (1998), 094030.

[31] M. Arima, S. Matsui and K. Shimizu, *Phys. Rev. C* **49** (1994), 2831.

[32] R. Bijker, F. Iachello and A. Leviatan, Phys. Rev. C **54**, 1935 (1996).

[33] R. Bijker, F. Iachello and A. Leviatan, Phys. Rev. D **55**, 2862 (1997).

[34] N. Kaiser, T. Waas and W. Weise, *Nucl. Phys. A* **612** (1997), 297.

[35] M.A.B. Bég, B.W. Lee and A. Pais, Phys. Rev. Lett. **13**, 514 (1964).

[36] S. Coleman and S.L. Glashow, Phys. Rev. Lett. **6**, 423 (1961).

[37] S.-T. Hong and G.E. Brown, Nucl. Phys. A **580**, 408 (1994).

[38] H.-C. Kim, M. Praszałowicz and K. Goeke, Phys. Rev. D **57**, 2859 (1998).

[39] I. Aznauryan, V.D. Burkert, T.-S.H. Lee and V. Mokeev, to be published in J. Phys.: Conf. Ser. (2011) [arXiv:1102.0597].

[40] V.D. Burkert, Preprint CEBAF-PR-88-012 (1988).

[41] I.G. Aznauryan *et al*, Phys. Rev. C **78**, 045209 (2008);
I.G. Aznauryan *et al*, Phys. Rev. C **80** 055203, (2009).

[42] M. Aiello, M. Ferraris, M.M. Giannini, M. Pizzo and E. Santopinto, Phys. Lett. B **387**, 215 (1996);
M. Aiello, M. M. Giannini and E. Santopinto, J. Phys. G: Nucl. Part. Phys. **24**, 753 (1998).

[43] L. Tiator, D. Drechsel, S. Kamalov, M.M. Giannini, E. Santopinto and A. Vassallo, Eur. Phys. J. A **19**, 55 (2004).

[44] S. Capstick and W. Roberts, Phys. Rev. D **49**, 4570 (1994).

[45] J. Ashman *et al*, Phys. Lett. B **206**, 364 (1988).

[46] S.D. Bass, *The spin structure of the proton* (World Scientific, Singapore, 2008).

[47] J. Speth and A.W. Thomas, Adv. Nucl. Phys. **24**, 83 (1998).

[48] B.S. Zou and D.O. Riska, Phys. Rev. Lett. **95**, 072001 (2005);
C.S. An, D.O. Riska and B.S. Zou, Phys. Rev. C **73**, 035207 (2006);
D.O. Riska and B.S. Zou, Phys. Lett. B **636**, 265 (2006);
Q.B. Li and D.O. Riska, Nucl.Phys. A **791**, 406 (2007).

[49] J.P.B.C. De Melo, T. Frederico, E. Pace and G. Salmé, Phys. Rev. D **73**, 074013 (2006);
J.P.B.C. De Melo, T. Frederico, E. Pace, S. Pisano and G. Salmé, Nucl. Phys. A **782**, 69c (2007); Phys. Lett. B **671**, 153 (2009).

[50] I. Guiasu and R. Koniuk, Phys. Rev. D **36**, 2757 (1987).

[51] P. Zenczykowski, Ann. Phys. (N.Y.) **169**, 453 (1986).

[52] R. Kokoski and N. Isgur, Phys. Rev. D **35**, 907 (1987).

[53] P. Geiger and N. Isgur, Phys. Rev. D **41**, 1595 (1990).

[54] P. Geiger and N. Isgur, Phys. Rev. D **47**, 5050 (1993).

[55] N. Isgur and J. Paton, Phys. Lett. B **124**, 247 (1983); Phys. Rev. D **31**, 2910 (1985).

[56] P. Geiger and N. Isgur, Phys. Rev. D **55**, 299 (1997).

[57] R. Bijker and E. Santopinto, Phys. Rev. C **80**, 065210 (2009).

[58] E. Santopinto and R. Bijker, Phys. Rev. C **82**, 062202(R) (2010).

[59] R. Bijker and E. Santopinto, J. Phys.: Conf. Ser. **239**, 012009 (2010).

[60] R. Bijker and E. Santopinto, J. Phys.: Conf. Ser. (2011), in press.

[61] W. Roberts and B. Silvestre-Brac, Few-Body Systems **11**, 171 (1992).

[62] B. Silvestre-Brac and C. Gignoux, Phys. Rev. D **43**, 3699 (1991).

[63] R. Marshak, S. Okubo and G. Sudarshan, Phys. Rev. **106**, 599 (1957);
S. Coleman and S.L. Glashow, Phys. Rev. Lett. **6**, 423 (1961).

[64] K. Gottfried, Phys. Rev. Lett. **18**, 1174 (1967).

[65] P. Amaudruz *et al*, Phys. Rev. Lett. **66**, 2712 (1991);
M. Arneodo *et al*, Nucl. Phys. B **487**, 3 (1997).

[66] A. Baldit *et al*, Phys. Lett. B **332**, 244 (1994).

[67] R.S. Towell *et al*, Phys. Rev. D **64**, 052002 (2001).

[68] K. Ackerstaff *et al*, Phys. Rev. Lett. **81**, 5519 (1998).

[69] Thomas A W 1983 *Phys. Lett.* B **126** 97 (1983);
E.M. Henley and G.A. Miller, Phys. Lett. B **251**, 453 (1990).

[70] E.J. Eichten, I. Hinchcliffe and C. Quigg, Phys. Rev. D **45**, 2269 (1992).

[71] Y.-J. Zhang, W.-Z. Deng and B.-Q. Ma, Phys. Rev. D **65**, 114005 (2002).

[72] M. Alberg, E.M. Henley, X. Ji and A.W. Thomas, Phys. Lett. B **389**, 367 (1996);
M. Alberg, T. Falter and E.M. Henley, Nucl. Phys. A **644**, 93 (1998).

[73] L. Shao, Y.-J. Zhang and B.-Q. Ma, Phys. Lett. B **686**, 136 (2010).

[74] R. Osipenko, private communication.

[75] A. Airapetian *et al*, Phys. Rev. D **75**, 012007 (2007).

[76] V.Yu. Alexakhin *et al*, Phys. Lett. B **647**, 8 (2007).

[77] F. Bradamante, Prog. Part. Nucl. Phys. **61**, 229 (2008).

[78] L.M. Sehgal, Phys. Rev. D **10**, 1663 (1974).

[79] P.G. Ratcliffe, Phys. Lett. B **192**, 180 (1987).

[80] F. Myhrer and A.W. Thomas, Phys. Lett. B **663**, 302 (2008).

[81] G.T. Garvey, arXiv:1001.4547 [nucl-th].

[82] R.L. Jaffe, Phys. Rev. D **54**, R6581 (1996).

[83] C. Boros and L. Zuo-tang, Phys. Rev. D **57**, 4491 (1998).

[84] D. Ashery and H.J. Lipkin, Phys. Lett. B **469**, 263 (1999).

[85] R. Bijker, *The structure of the nucleon: baryons and pentaquarks*, Lecture notes of the *IV Escuela Mexicana de Física Nuclear*, Eds. E.F. Aguilera, E. Hernández and J. Hirsch, (Mexico City, 2005), 138-165 [arXiv:nucl-th/0504079].

[86] R. Koniuk and N. Isgur, *Phys. Rev. D* **21** (1980), 1868.

[87] J.J. de Swart, Rev. Mod. Phys. **35**, 916 (1963).

[88] S. Godfrey and N. Isgur, Phys. Rev. D **32**, 189 (1985).